

# **The role of the E2 copper binding domain in the cell biology of the amyloid precursor protein**

Sophee Blanthorn-Hazell BSc. (Hons)

A thesis submitted to the University of Lancaster for the degree of

Master of Science

(By Research) in Biomedical Science

Supervised by Dr Edward Parkin

October 2014

Division of Biomedical Life Sciences

Faculty of Health and Medicine

Lancaster University



## **Declaration**

I declare that this thesis is my own work submitted for the degree of Masters (by Research) in Biomedical Science at Lancaster University.

This work has not been previously submitted to another University or Institute of Learning for the award of a higher degree.

## **Acknowledgements**

First and foremost I would like to thank Dr Edward Parkin and Dr Craig Delury for their immeasurable support, advice and constructive criticism during the completion of this project. Without their help I could not have finished this challenging year.

I would also like to extend my thanks to Professor David Allsop and Dr Paul McKean for their guidance and advice throughout the year, and to Michelle Bates and Jane Andre for their unparalleled technical advice on the practicalities of this project.

I am extremely grateful to the Liz and Terry Bramall Charitable Trust for their funding, without which this project would not have been possible

Finally, I am indebted to my family, friends and to my partner, Gregory Herneman, for the vast emotional support and advice they have provided over the last year. The completion of this project is owed to them.

# Abstract

Alzheimer's disease is a neurodegenerative disorder characterised by the accumulation, in the brain, of neurotoxic amyloid beta-(A $\beta$ ) peptides. These peptides are generated from the amyloid precursor protein (APP) via the amyloidogenic proteolytic pathway which also leads to the formation of soluble APP beta (sAPP $\beta$ ). Alternatively, APP can be cleaved by the non-amyloidogenic pathway in which an  $\alpha$ -secretase activity cleaves the protein within the A $\beta$  region generating soluble APP alpha (sAPP $\alpha$ ). APP itself binds to copper at a number of sites, including a recently identified E2 copper binding domain (E2 CuBD) within the extracellular region of the protein. The current project aims were to investigate how copper binding within the APP E2 CuBD might influence the expression, proteolysis, cellular localisation and cytotoxicity of APP. In order to achieve this, a range of E2 CuBD mutants were generated in which various metal-co-ordinating histidine residues were mutated to alanine. These constructs were expressed in HEK and SH-SY5Y cells and the effects of the mutations on the afore mentioned properties of APP were assessed. The results show that these mutations had little consistent effect on the expression, proteolysis or cellular localisation of APP. Furthermore, whilst wild-type APP accentuated copper-mediated cytotoxicity in HEK and SH-SY5Y cells, mutating the histidine residues in the E2 domain of the protein had little effect on this phenomenon. Thus, it would appear that copper binding to the E2 domain of APP is, most likely, not an important event in the pathogenesis of Alzheimer's disease.

## Contents

Abstract	4
Abbreviations	9
1. Introduction	11
1.1. Introduction	12
1.1.1. History	12
1.1.2. Pathological hallmarks of the disease	13
1.1.3. Symptoms	14
1.1.4. Diagnosis	14
1.1.5. Treatment	15
1.1.6. Prognosis	16
1.2. Etiology and genetics of Alzheimer's disease	17
1.2.1. Etiology	17
1.2.2. Genetics	20
1.3. The amyloid precursor protein	22
1.3.1. APP trafficking and proteolysis	23
1.4. The physiological roles of APP and its derivatives	28
1.4.1. Full-length APP and sAPP $\alpha$	28
1.4.2. AICD	29
1.4.3. A $\beta$ -peptides	30
1.5. Copper, Alzheimer's disease and APP	30
1.5.1. Copper and Alzheimer's disease	32
1.5.2. Copper and APP expression	33
1.5.3. Copper and APP proteolysis / trafficking	34
1.5.4. APP and the regulation of copper toxicity	34
1.5.5. APP and A $\beta$ aggregation / clearance	35
1.5.6. Copper and the mediation of A $\beta$ neurotoxicity	36
1.5.7. APP as a copper binding protein	37
1.6. Aims of the current project	38
2. Materials and Methods	40
2.1. Materials	41
2.2. Methods	41
2.2.1. Bacterial transformation	41

2.2.2.	Preparation of agar plates and bacterial culture .....	41
2.2.3.	DNA purification .....	42
2.2.4.	Ethanol precipitation of DNA .....	42
2.2.5.	Mammalian cell culture .....	43
2.2.6.	Transient transfection of HEK cells.....	43
2.2.7.	Stable transfection of HEK and SH-SY5Y cells.....	44
2.2.8.	Preparation of cell lysates and conditioned medium samples.....	45
2.2.9.	Bicinchoninic acid (BCA) protein assay .....	46
2.2.10.	Sodium dodecylsulphate-polyacrylamide gel electrophoresis (SDS-PAGE) ..	47
2.2.11.	Western blotting.....	49
2.2.12.	Stripping and re-probing immunoblots for anti-actin .....	50
2.2.13.	Copper toxicity assays .....	51
2.2.15.	Immunofluorescence.....	51
2.2.16.	Statistical analysis.....	52
3.	Results	53
3.0	Introduction.....	54
3.1.	Transient expression and proteolysis of constructs in HEK cells .....	54
3.2.	Stable expression and proteolysis of constructs in HEK cells .....	58
3.3.	Stable expression and proteolysis of constructs in SH-SY5Y cells.....	61
3.4.	Subcellular localisation of constructs in stable SH-SY5Y transfectants.....	65
3.5.	Role of the APP E2 CuBD in cytotoxicity.....	68
3.5.1.	Free copper-mediated neurotoxicity .....	68
3.5.2.	Copper-glycine-mediated neurotoxicity.....	72
3.6.	Summary .....	78
4.	Discussion	80
4.1.	Discussion.....	81
4.1.1.	APP expression .....	81
4.1.2.	APP proteolysis.....	82
4.1.3.	APP localisation.....	84
4.1.4.	Copper-mediated cytotoxicity.....	85
4.2.	Conclusions and future directions.....	88
5.	References	89

## Figures

Figure 1.1. Microscopic pathology of the AD-afflicted brain showing large dense-core senile plaques and neurofibrillary tangles. ....	13
Figure 1.2. Schematic diagram of APP (numbering according to APP <sub>770</sub> ) .....	23
Figure 1.3. APP trafficking (A) and proteolysis (B) .....	24
Figure 1.4. Simplified uptake of copper into cells. ....	31
Figure 3.1. A schematic diagram of APP <sub>695</sub> showing the location of the residues mutated in the current study.....	55
Figure 3.2. APP expression levels in transiently transfected HEK cell lysate.....	56
Figure 3.3. sAPP $\alpha$ levels in medium from transiently transfected HEK cells. ....	57
Figure 3.4. APP expression levels in stably transfected HEK cell lysates .....	59
Figure 3.5. sAPP $\alpha$ and sAPP $\beta$ levels in medium from stably transfected HEK cells.....	60
Figure 3.6. APP expression levels in stably transfected SH-SY5Y cell lysates. ....	63
Figure 3.7. sAPP $\alpha$ and sAPP $\beta$ levels in medium from stably transfected SH-SY5Y cells .....	64
Figure 3.8. Immunofluorescence detection of APP expression in SH-SY5Y stable transfectants. ....	67
Figure 3.9. The effect of free copper on the viability of HEK cell stable transfectants .....	70
Figure 3.10. The effect of free copper on the viability of SH-SY5Y cell stable transfectants. ....	70
Figure 3.11. The effect of glycine-complexed copper on the viability of mock-transfected HEK cells. ....	73
Figure 3.12. The effect of glycine-complexed copper on the viability of HEK cell stable transfectants .....	74
Figure 3.13. The effect of glycine-complexed copper on the viability of mock-transfected SH-SY5Y cells.....	76
Figure 3.14. The effect of glycine-complexed copper on the viability of SH-SY5Y cell stable transfectants .....	77

## Tables

Table 1.1. Results of a meta-analysis examining the effects of cholinesterase inhibitors on cognition versus placebo. ....	16
Table 1.2 The most prevalent gene-disease association risks in late-onset AD.....	22
Table 1.3. AICD target genes. ....	16
Table 2.1. BSA standards and their loading in 96 well plates. ....	47
Table 2.2. SDS-PAGE resolving and stacking gel constituents. ....	48
Table 2.3. Antibody dilutions for Western blotting. ....	50

# Abbreviations

**ADAM** A disintegrin and metalloproteinase

**AICD** APP intracellular domain

**APP** Amyloid precursor protein

**APP-E1 CuBD** Amyloid precursor protein E1 copper binding domain

**APP-E2 CuBD** Amyloid precursor protein E2 copper binding domain

**A $\beta$**  Amyloid beta

**BACE1** Beta-site APP-cleaving enzyme 1

**BCA** Bicinchoninic acid assay

**BSA** Bovine Serum Albumin

**CNS** Central nervous system

**CSF** cerebrospinal fluid

**CTF-83** C-terminal fragment of 83 amino acids

**CTF-99** C-terminal fragment of 99 amino acids

**CTR1** Copper plasma membrane transporter 1

**DAPI** 4', 6-diamidino-2-phenylindole

**DMSO** dimethyl sulfoxide.

**ER** Endoplasmic reticulum

**GFD** Growth factor domain

**GWAS** Genome-Wide Association Studies

**HBD** Heparin binding domain

**HEK** Human embryonic kidney

**KPI** Kunitz-type protease inhibitor

**LB** Liquid broth

**LRP1** low density lipoprotein receptor-related protein 1

**NCT** Nicastrin

**PBS** Phosphate buffered saline

**PBS-TWEEN** Phosphate buffered saline + 0.1% (v/v) TWEEN-20

**PEN2** Presenilin enhancer 2

**PSEN1** Presenilin 1

**PSEN2** Presenilin 2

**sAPP $\alpha$**  soluble APP alpha

**sAPP $\beta$**  soluble APP beta

**SDS-PAGE** Sodium dodecylsulphate-polyacrylamide gel electrophoresis

**Wt-APP** Wild-type APP

**ZMP** Zinc metalloprotease

# **1. Introduction**

## **1.1. Introduction**

Dementia is a generic term for diseases which involve neuronal death or malfunctioning, resulting in decreased cognitive and functional abilities (manifested as detrimental alterations in behaviour, language and memory) [5]. Alzheimer's disease (AD) is a progressive neurodegenerative condition that is estimated to be responsible for 60-80% of all dementia cases worldwide. In 2006, the prevalence of AD was 26.5 million worldwide; in an ageing population this number is set to increase dramatically with projections estimated at 106 million by 2050 [6]. The cost of AD to the UK economy is an estimated £23 billion per year with each dementia patient costing the economy £28,000 per annum.

### **1.1.1. History**

In 1907, Alois Alzheimer used silver staining to demonstrate the presence of neurofibrillary tangles (NFTs) (later shown to consist of aggregated tau protein) and senile plaques within the post-mortem brain of a 55 year old woman who had suffered from memory loss, delusions and a decline in cognitive ability [7]; his co-worker, Emile Kraepelin, subsequently named the condition Alzheimer's disease. It was initially thought that plaques and tangles were specific to AD but this was disputed when senile plaques and NFTs were identified in 84% and 97% of ageing brains respectively, (reviewed in [8]), suggesting that they were a common feature of ageing. These pathological hallmarks were only definitively associated with dementia in 1968 when Blessed *et al.* [8] demonstrated a strong correlation between plaque burden and dementia scores.

### 1.1.2. Pathological hallmarks of the disease

Two key pathological hallmarks are associated with the AD-afflicted brain; neurofibrillary tangles and senile plaques (Fig. 1.1). NFTs are formed intracellularly when the hyperphosphorylated form of the microtubule-associated protein, tau, misfolds and relocates to the neuronal soma from the neuronal microtubules. The damaged dendrites of neurons that have died as a result of tangle formation degrade to form neoprill threads (Fig 1.1) [9]. The loss of normal tau functioning and neuronal degeneration are thought to inhibit normal axonal transport and contribute to cerebral atrophy [10].

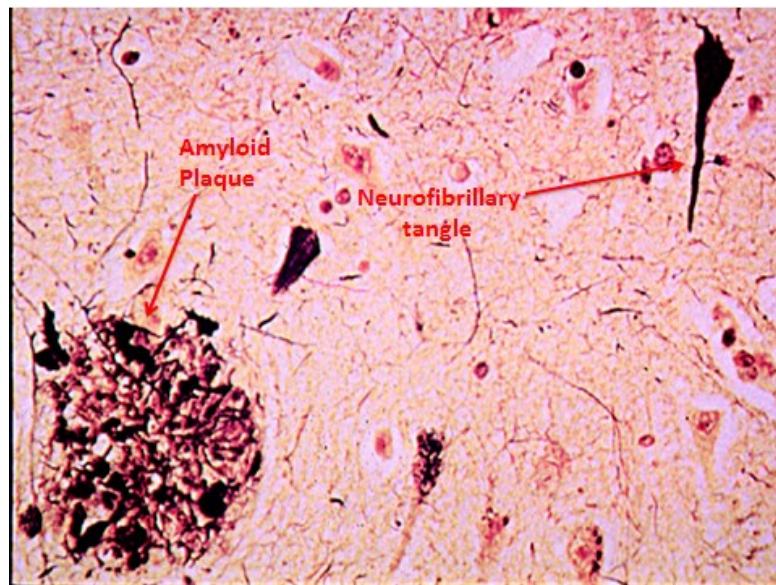


**Figure 3.1. Microscopic pathology of the AD-afflicted brain showing large dense-core senile plaques and neurofibrillary tangles.** Adapted from Bird [11].

The extracellular dense-core senile plaques in the AD-afflicted brain comprise mainly of amyloid beta ( $A\beta$ )-peptides. These peptides aggregate first to form early oligomers before assembling into the mature plaques [9]. Whether it is the mature plaques or the early oligomers that form the neurotoxic entities in AD is the subject of some debate [12, 13]

Many studies have shown that both A $\beta$ -peptides and NFTs are neurotoxic and that their regional distribution within the brain correlates with the symptoms manifested in AD (reviewed in [9]). However their role in disease pathogenesis has also been questioned as a result of their presence in the normal aged brain (reviewed in [14] and [15]).

### **1.1.3. Symptoms**

AD is often preceded by the onset of mild cognitive impairment (MCI) which is defined as a decline of cognitive function greater than expected for an individual's age and educational background [16]. It has been shown that 22% of individuals diagnosed with MCI progressed to some form of dementia over a three year period [17], although specific studies on AD have demonstrated a range of progression rates from 11-33% over two years and that a diagnosis of MCI does not necessarily mean a certain progression to AD [16]. The progression of symptoms from MCI to severe dementia is described in the global deterioration scale (GDS) by Reisberg *et al.* [18]. MCI is described as a loss of memory noticeable to family and friends, where the individual may lose important items or struggle to retain information. As MCI progresses to moderate dementia, the individual often struggles to recall the date and previous memories, cope with day-to-day life and dress appropriately. Ultimately the dementia progresses to the severe criteria for which symptoms include; major behavioural disruptions, an inability to recognise loved ones and incontinence, with a complete loss of psychomotor skills and speech [18].

### **1.1.4. Diagnosis**

In the UK, a diagnosis of AD begins with the exclusion of other possible conditions. Clinical cognitive assessments are used to measure cognition, function and

behaviour. Most frequently, a lower than average score in the Mini Mental State Examination (MMSE) is used to diagnose dementia. Following this, structural imaging such as magnetic resonance imaging or computed tomography would then be used in order to determine the specific subtype of dementia [19]; AD is generally defined by atrophy in the temporal lobes and hippocampus.

#### **1.1.5. Treatment**

Current therapies approved by the UK drugs regulatory agency target the neurotransmitter dysfunction observed in AD. Cholinesterase inhibitors, prescribed during early- to mid-AD, reduce the degradation of acetylcholine in the synaptic cleft. The three cholinesterase inhibitors currently recommended by the National Institute for Health and Care Excellence (NICE) for the treatment of cognitive symptoms include donepezil, galantamine and rivastigmine [19]. However, a meta-analysis of these treatments demonstrated only a modest improvement in function, cognition and behaviour compared with placebo (summarised in Table 1.1) [20].

Memantine is a non-competitive N-methyl-D-aspartate (NMDA) receptor antagonist postulated to protect neurons against toxicity mediated by excess glutamatergic activity. Benefits of memantine include improvements in long term potentiation and decreased tau hyperphosphorylation (reviewed in [21] ). Like the acetylcholinesterase inhibitors, the effects of memantine on cognition are modest and

only significant during the later stages of AD [21]. Neither therapeutic approach cures AD or changes disease progression and outcome.

**Table 1.1. Results of a meta-analysis examining the effects of cholinesterase inhibitors on cognition versus placebo.** Adapted from Hanson *et al.* [20].

	<b>Test</b>	<b>Test scale</b>	<b>Average weighted mean difference vs placebo</b>
<b>Cognitive decline</b>	Alzheimer’s Disease Assessment Scale (ADAS)-Cognitive	70 point scale with higher scores translating as more severe cognitive defects	-2.81
<b>Behaviour</b>	Neuropsychiatric Inventory (NPI)	144 point scale with higher scores translating as more severe behavioural changes	-2.79
<b>Normal functioning</b>	Multiple measures of function used	Mean changes and standard deviations of individual tests combined. Increased values translate as improved functioning	0.28

### 1.1.6. Prognosis

As a result of late diagnosis and a lack of effective treatments, the prognosis of AD is poor. Median survival after diagnosis has been estimated at 4.2 years in men and 5.7 years in women. The MMSE score at diagnosis is an effective marker of survival [22]. As neurodegeneration starts to affect the pre-and postcentral gyri, frontal operculum and Rolandic operculum of the brain, the patient loses the ability to swallow [23]. Malnutrition, infection and aspiration pneumonia are common causes of death in patients, as are urinary tract infections caused by the degeneration of regions of the brain responsible for bladder control. The relative risks of pneumonia/bronchitis and infectious disease in individuals with AD are 2.26 and 1.51 compared with age-matched controls [24].

## **1.2. Etiology and genetics of Alzheimer's disease**

### **1.2.1. Etiology**

The definitive cause of progressive neural damage observed during AD has yet to be determined although there are four key hypotheses in this respect; the vascular theory, the tau theory, the oxidative stress theory and the amyloid cascade theory.

#### The vascular theory

The vascular theory of AD proposes that altered cerebrovascular systems in the body caused by both age and vascular disorders are the major cause of AD. The altered systems create vascular uncoupling and cerebral hypoperfusion which in turn stimulate abnormal angiogenesis, endothelial death and oxidative stress in the vascular systems of the brain. Ultimately, the compromised blood brain barrier (BBB) and reduced cerebral blood flow lead to synaptic injury and neuronal atrophy, which induce MCI and dementia [25]. The compromised BBB may further lead to ineffective clearance of A $\beta$  due to changes in transport proteins such as low density lipoprotein receptor related protein-1 (LRP1) [26]. Several lines of evidence support this theory as the major etiological cause of AD. Individuals with atherosclerosis, which reduces cerebral blood flow, are at increased risk of AD which is potentiated by the severity of the atherosclerosis [27]. In addition, mutant murine models of diminished A $\beta$  clearance across the BBB, which occurs when the BBB is compromised, exhibit increased plaque number and deposition increased neurotoxicity [28].

#### The tau theory

The tau theory proposes that the hyperphosphorylation of the microtubule-associated tau protein induces the neurotoxicity and degeneration in AD. Studies have

demonstrated that tau hyperphosphorylation can be caused by increasing A $\beta$  levels, dysregulation of phosphorylation or abnormal glucose metabolism (reviewed in [29]). The hyperphosphorylated tau loses its normal biological activity, and polymerises to form NFTs. Soluble hyperphosphorylated tau has also been shown to be neurotoxic causing neuronal atrophy, impaired axonal transport and compromised microtubule networks [29]. Recent research suggests that tau abnormalities occur downstream of A $\beta$  accumulation and that increasing cerebral A $\beta$  levels may initiate the formation of NFTs [10].

A core finding in support of the tau theory of AD is that NFT distribution within the brain mirrors AD neuropathology more closely than A $\beta$  plaques [9]. Further support has been shown by Roberson *et al.* [30] who demonstrated that mice overexpressing APP (APP $+/+$ ) exhibited significant difficulties in spatial learning and memory compared to WT mice. The authors also showed that knocking out endogenous tau in APP  $+/+$  mice returned spatial learning and memory scores to those observed in wild-type mice. Knocking out tau did not affect A $\beta$  levels, suggesting that tau, rather than A $\beta$  may be the cause of neurodegeneration in AD. More recently, it has been shown that sequestration of zinc by A $\beta$  plaques reduces intra-neuronal zinc available to tau which subsequently destabilises microtubules [31]. This also provides a potential link between A $\beta$  and tau neurotoxicity.

#### The oxidative stress theory of AD

Oxidative stress was initially proposed as a cause of AD due to its involvement in the pathophysiology of other diseases including Parkinson's, Down's syndrome and amyotrophic lateral sclerosis [32]. It is proposed that reactive oxygen species (ROS) generated from a number of processes including ageing and the reduction of metals in

amyloid plaques cause peroxidation of cell membrane polyunsaturated fatty acids. ROS can be generated both outside the cell through environmental factors, and inside the cell via membrane bound, mitochondrial or cytosolic factors. In the presence of redox metals, hydrogen peroxide also undergoes Fenton's chemistry to produce hydroxyl radicals [33]. ROS damage the cell membrane and mitochondria, and disturb Na/K ATPase's which increase intracellular calcium leading to cell death and further free radical generation [32]. This irreversible damage to cells is postulated to cause the neuronal atrophy observed in AD.

Epidemiological studies have revealed that markers of lipid peroxidation are significantly higher in AD brains than age-matched controls and oxidative stress markers are perturbed early in the disease (reviewed in [34]) which support a role of oxidative stress in the pathogenesis of AD. *In vitro* studies have found increased peroxidation markers in cells exposed to copper which correlates with cell toxicity [35]. Furthermore, a randomised controlled trial of 341 patients found that those who received the antioxidant vitamin E exhibited significant delays in the time until institutionalisation, death or severe dementia relative to placebo [36]. This supports an *in vivo* role of oxidative stress in the pathogenesis of AD.

#### The amyloid cascade theory

The amyloid cascade hypothesis is the most well acknowledged etiological theory of AD. This is due to early studies identifying that all early-onset familial AD (EOFAD) mutations disrupt normal APP processing (reviewed in [37]). It proposes that altered processing of APP or decreased A $\beta$  clearance results in increased A $\beta$  aggregation in the extracellular space of the brain. The updated hypothesis proposes that soluble A $\beta$  oligomers, over A $\beta$  plaques, induce toxic stress. This has been

supported by studies showing significantly increased toxicity of A $\beta$  oligomers compared to A $\beta$  fibrils [38, 39].

Oligomeric A $\beta$  has been shown to recruit inflammatory cytokines which induces oxidative stress [40]. This, in turn, is hypothesised to generate NFTs, synaptic failure and AD pathology (reviewed in [13]). The theory further suggests that an increased ratio of A $\beta$ 42 to A $\beta$ 40 (A $\beta$ 42/A $\beta$ 40) generation is a major factor in AD neuropathology. This is supported by studies showing that A $\beta$ 42 increases plaque formation and neurotoxicity relative to A $\beta$ 40, although both exhibit significant toxicity to neurons *in vitro* [41]. In addition, dementia in individuals carrying the PSEN1 mutation ( see section 1.2.2) progresses in a positive correlation with the A $\beta$ 42/A $\beta$ 40 ratio [42]. Epidemiological studies have demonstrated that A $\beta$ -plaques correlate strongly with cognitive decline in the entorhinal cortex [43]. Taken together, these studies strongly support a role for the A $\beta$  peptide in AD pathogenesis and progression.

### **1.2.2. Genetics**

The first genetic mutation causing EOFAD was found on chromosome 21 in the allele encoding the amyloid precursor protein (*APP*) [44]. The mutation, found in a British pedigree known as F23, consists of a dominant mis-sense mutation at position 717 of *APP* and is referred to as the V717I (*APP*<sub>770</sub> numbering) mutation. This mutation leads to aberrant APP processing through altering  $\gamma$ -secretase cleavage and increasing the A $\beta$ 42/A $\beta$ 40 ratio [45]. More recently, a study by Muratore *et al.* [46] used neurons taken from inducible pluripotent cells of mutation carriers to show that the V717A mutation also alters the subcellular localisation of APP and the total and phosphorylated levels of tau.

Generally, EOFAD-associated mutations enhance the generation of toxic A $\beta$ -peptides from the APP protein through altered  $\gamma$ -secretase action that increases the amount of A $\beta$ 42 peptide production relative to A $\beta$ 40 [45] (see section 1.3.1). Some mutations can also affect *APP*, although these are rare with only 16 recognised *APP* mutations identified to date (reviewed in [37]).

EOFAD-associated mutations in  $\gamma$ -secretase have been located on chromosomes 14 and 1 within the alleles encoding the  $\gamma$ -secretase components presenilins 1 and 2 (PS1 and PS2), respectively. Individuals carrying PS1 or PS2 mutations exhibit either overall increased A $\beta$  generation or an increase in the A $\beta$ 42/A $\beta$ 40 ratio supporting a ‘gain of function’ hypothesis [37]. A missense mutation in PS1 has also been shown to inhibit the autoproteolysis of the protein required for the subsequent formation of the enzymatically active heterodimer [47].

EOFAD-associated mutations are only present in approximately 0.1% of all AD cases, the remainder of them representing sporadic forms of the disease [37]. Recent Genome-Wide Association Studies (GWAS) have highlighted several genes that confer increased or decreased susceptibility to AD and these are summarised in Table 1.2. The Apolipoprotein E (ApoE) gene seems to be most closely linked to sporadic AD with inheritance of the  $\epsilon$ 4 allele being closely associated with disease development [48].

**Table 2.2 The most prevalent gene-disease association risks in late-onset AD.** OR; odds ratio, SNP; single nucleotide polymorphism Adapted from Sleegers et al[2] and Guerreiro[3]

Gene/locus	Protein	Polymorphisms	OR of most severe SNP	Effect on amyloid pathway	Other functions
<b>APOE</b>	Apolipoprotein E	Apoε ε2/3/4	3.57	Clearance, fibril formation	Immune response, lipid metabolism
<b>CLU</b>	Clusterin	Rs11136000	0.85	Clearance, fibril formation	Immune response, lipid metabolism
<b>CST3</b>	Cystatin c	rs1064039	1.13	Amyloid angiopathy	Atherosclerosis
<b>IL1B</b>	Interleukin 1, beta	rs1143634	1.17		Active cytokine
<b>PICALM</b>	Phosphatidylinositol binding clathrin assembly protein	Rs541458	0.87	Recycling APP	
<b>TNK1</b>	Tyrosine kinase, non-receptor, 1	rs1554948	0.86		Phospholipid signal transduction
<b>TFAM</b>	Transcriptional factor a, mitochondrial	rs2306604	0.82		
<b>ACE</b>	Angiotensin-converting enzyme	Rs1800764	0.83		Cardiovascular pathophysiology
<b>TREM2</b>	Microglial transmembrane glycoprotein	rs75932628-T	4.5	Clearance	Immune response

### 1.3. The amyloid precursor protein

The first isolation of APP was in 1987 when Kang *et al.* [49] successfully isolated full length APP cDNA through using foetal mRNA and probing for the N-terminus of the  $\beta$ -amyloid protein. APP is a single-pass, multi-domain, transmembrane protein. Alternate splicing of exons 7, 8 and 15 of the *APP* gene generates at least ten known isoforms of the protein; the most common of which are 695, 751 and 770 residues long [50]. APP<sub>695</sub> is expressed principally in the central nervous system (CNS) at levels around 6-10 times greater than the APP<sub>751</sub> and APP<sub>770</sub>

isoforms, which are expressed in both the CNS and peripheral tissue [51]. Unlike APP<sub>751</sub> and APP<sub>770</sub>, APP<sub>695</sub> lacks a Kunitz-type protease inhibitor (KPI) domain (Fig. 1.2).

The structure of APP comprises a large extracellular domain, a transmembrane region and a short C-terminal intracellular domain (Fig. 1.2). Within the extracellular domain of the protein there is a conserved E1 domain containing a cysteine-rich growth factor / heparin binding domain (GFD / HBD) and a copper binding domain [52]. This is followed by an acidic domain, the KPI region and the E2 domain. The E2 domain contains a second heparin binding site [52] which evidence suggests is responsible for synaptic growth and stabilisation [53].

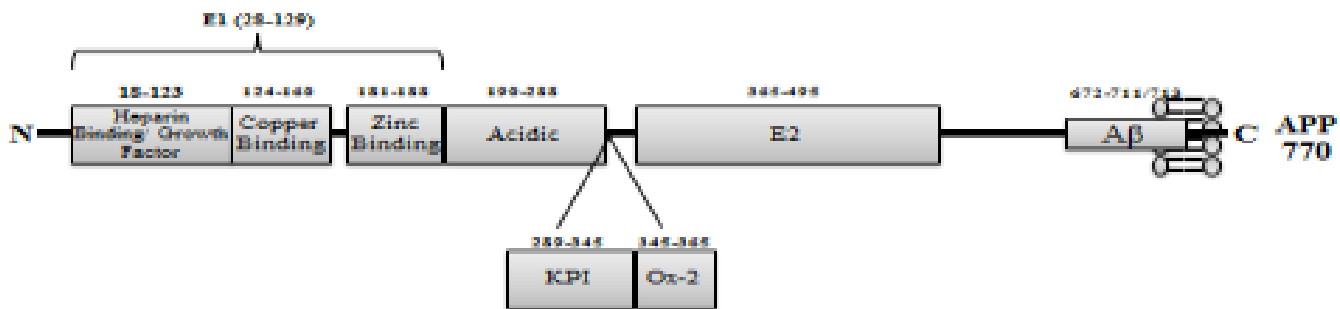


**Figure 1.4. Schematic diagram of APP (numbering according to APP<sub>770</sub>).** APP<sub>695</sub> does not exhibit a KPI or OX2 domain, whilst APP<sub>751</sub> does not exhibit an OX2 domain. Adapted from Duce *et al.* [1].

### 1.3.1. APP trafficking and proteolysis

APP is synthesised on the endoplasmic reticulum (ER) and transported through the Golgi apparatus where it undergoes post-translational modifications including O-glycosylation and sulfation [54] before being transported to the neuronal axon (Fig. 1.3A). The protein then undergoes fast anterograde transport to the synapse. Only around 10% of APP reaches the plasma membrane from the trans-Golgi network with most of the protein being proteolytically shed from the cell surface and

the remainder being re-internalised to lysosomes or early endosomes via targeting to clathrin-coated pits involving the YENPTY motif within the APP cytosolic domain [55].

Proteolysis of APP occurs through two major routes; the amyloidogenic and non-amyloidogenic pathways [56] (Fig. 1.3B). The amyloidogenic pathway comprises of  $\beta$ -secretase cleavage generating the soluble ectodomain sAPP $\beta$ , and a membrane anchored C-terminal fragment of 99 amino acids (CTF-99) (Fig. 3B). The latter

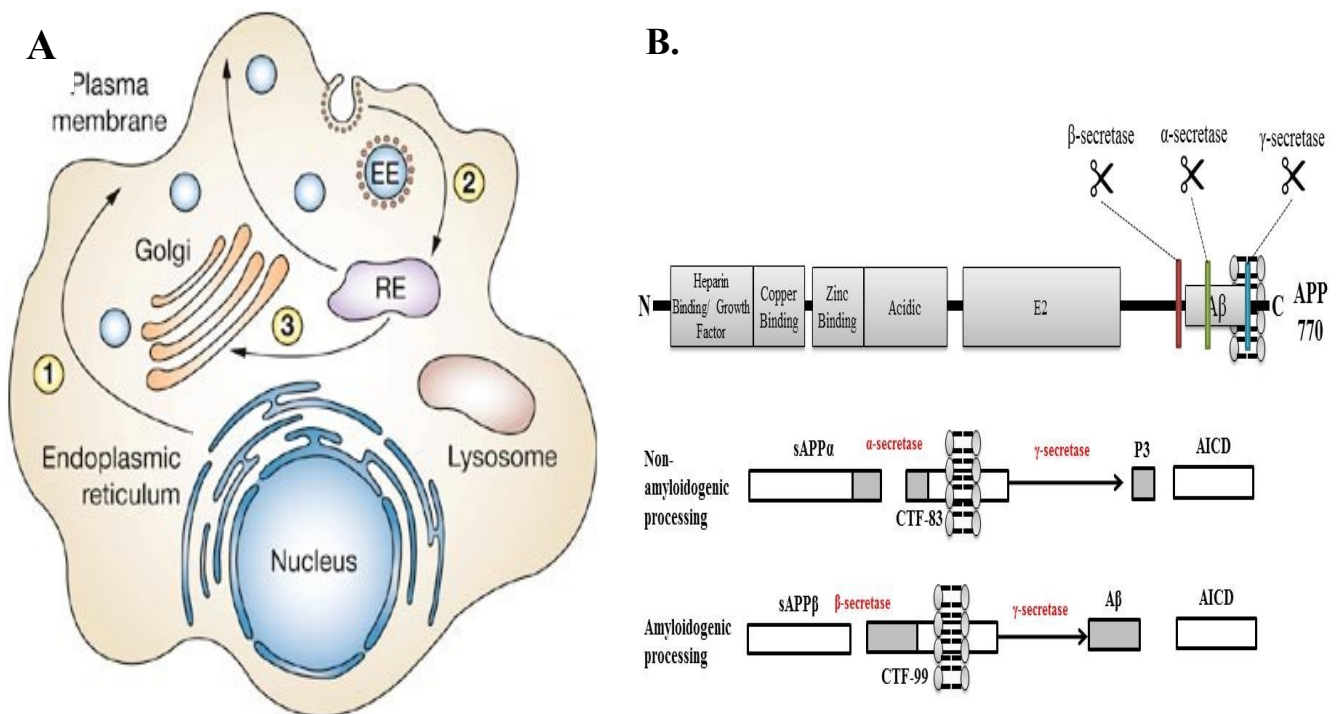


**Figure 1.3. APP trafficking (A) and proteolysis (B).** (A) Taken from Cheng *et al* [57]. (1) APP is synthesised in the endoplasmic reticulum, then matures along the secretory pathway through the Golgi. Once it reaches the cell surface, APP is either processed by the non-amyloidogenic  $\alpha$ -secretase or (2) re-internalised to the endosomal compartments. Most amyloidogenic processing occurs in the endosomal compartments by BACE. (3) The remaining APP is recycled to the Golgi or degraded in the lysosomes. (B) The amyloidogenic and non-amyloidogenic processing of APP. During non-amyloidogenic processing, APP is cleaved by  $\alpha$ -secretase within the A $\beta$  domain creating a membrane anchored CTF-83 fragment and sAPP $\alpha$ . CTF-83 is subsequently cleaved within the membrane by  $\gamma$ -secretase, which generates the intracellular AICD and the extracellular p3 fragment. During amyloidogenic processing, APP is cleaved by  $\beta$ -secretase generating the membrane anchored CTF-99 and sAPP $\beta$ . CTF-99 is subsequently cleaved by  $\gamma$ -secretase, releasing the AICD intracellularly and the toxic A $\beta$  fragment extracellularly.

fragment is then cleaved by a  $\gamma$ -secretase complex to yield the neurotoxic A $\beta$ -peptides characteristic of AD and the APP intracellular domain (AICD). Alternatively, in the non-amyloidogenic pathway, APP is cleaved by an  $\alpha$ -secretase activity generating a soluble ectodomain (sAPP $\alpha$ ) and a membrane anchored C-terminal fragment of 83 amino acids (CTF-83).

#### ***1.3.1.1. $\beta$ -secretase***

The enzyme responsible for the  $\beta$ -secretase processing of APP was isolated almost simultaneously by several groups [58-60] and is now unilaterally referred to as beta-site APP-cleaving enzyme 1 (BACE1). APP is cleaved by the  $\beta$ -secretase BACE1 C-terminal to methionine 596 (APP<sub>770</sub> numbering) [58]. Vassar *et al.* [58] used a cDNA library to identify BACE1 as a type-1 transmembrane aspartyl protease with an active site on the luminal side of the membrane. The same author used immunoblotting to reveal that BACE1 was predominantly localised to the Golgi and endosomes, whilst it was detected at low levels in lysosomes and the ER. Cells overexpressing BACE1 exhibited a two-fold increase in A $\beta$  production and a significant decrease in the yield of sAPP $\alpha$  [58]. The *in vivo* role of BACE1 as a  $\beta$ -secretase was subsequently confirmed through the use of BACE1 knockout mice which exhibited decreased A $\beta$  generation with a reciprocal increase in sAPP $\alpha$  production [61].

#### ***1.3.1.2. $\gamma$ -secretase***

The C99 fragment generated by  $\beta$ -secretase processing of APP is then cleaved by the  $\gamma$ -secretase complex at a number of possible positions within the C-terminal

region of the A $\beta$  domain [50]. The  $\gamma$ -secretase is a multi-protein complex consisting of presenilin 1 or 2 (PS1 or PS2), nicastrin (NCT), Aph1 and presenilin enhancer 2 (PEN2) [50].

PS undergoes autocatalytic proteolysis to generate N- and C-terminal fragments that subsequently form an active heterodimer in which the two aspartyl residues of the active site are spatially arranged in the correct orientation for the cleavage of the APP substrate [47]. Whilst this heterodimer carries the active protease component of the  $\gamma$ -secretase complex, NCT, Aph1 and PEN2 bind to the complex regulating its conformation and, therefore, activity [62].

Amongst other transmembrane substrates,  $\gamma$ -secretase complexes are also responsible for the proteolysis of Notch receptors; in fact the parallels between APP and Notch proteolysis originally led to the proposal of a signalling role for the AICD [62, 63]. The AICD has subsequently been shown to alter the expression of a range of proteins including APP itself (discussed in more detail in section 1.4.2.).

The subcellular localisation of  $\gamma$ -secretase-mediated APP proteolysis remains controversial although recent research using green fluorescent protein-tagged APP has demonstrated that the bulk of this processing occurs in the early endosomes or surface membrane with little activity in the early secretory pathway [63]. An important regulatory aspect of both  $\beta$ - and  $\alpha$ -secretase APP processing is the co-localisation of the enzymes and substrate within lipid rafts. These are areas of the membrane enriched in cholesterol, saturated fatty acids and phospholipids such as phosphatidylinositol and phosphatidylserine carrying saturated fatty acyl chains [64, 65]. In fact, multiple groups have demonstrated a role for lipid rafts in the amyloidogenic processing of APP (reviewed in [66]).

### ***1.3.1.3. $\alpha$ -secretase***

The  $\alpha$ -secretase activity cleaves APP between lysine 16 and leucine 17 of the A $\beta$  domain thereby precluding the formation of intact neurotoxic peptides. The first clues as to the identity of the enzyme came when Roberts *et al.* [67] used a crude membrane preparation to determine that  $\alpha$ -secretase was an integral membrane protease and a member of the zinc metalloprotease (ZMP) family. Subsequently, several members of the ADAM (a disintegrin and metalloproteinase) subgroup of ZMPs have been implicated as possible  $\alpha$ -secretases including ADAMs 9, 10 and 17 (reviewed in [56]). Perhaps the most widely implicated of these is ADAM10 which exhibits both basal and regulated (i.e. phorbol ester-stimulated)  $\alpha$ -secretase activity [68]. Postina *et al.* [69] found an increase in sAPP $\alpha$  levels with a subsequent decrease in sAPP $\beta$  and A $\beta$  plaques in mice overexpressing ADAM10, providing the first *in vivo* evidence that ADAM10 is the primary  $\alpha$ -secretase. The same study showed a reverse of these results in mice expressing inactive ADAM10. In humans, low levels of ADAM10 expression in platelets are associated with low cerebrospinal fluid (CSF) levels of sAPP $\alpha$  in AD patients [70].

Early research into the non-amyloidogenic processing of APP indicated that  $\alpha$ -secretase was located within the plasma membrane and that APP must travel to the cell surface before undergoing non-amyloidogenic proteolysis [71]. Whilst the cell surface is still considered the major site of  $\alpha$ -secretase activity, small amounts have been observed in the trans-Golgi network [68].

## 1.4. The physiological roles of APP and its derivatives

### 1.4.1. Full-length APP and sAPP $\alpha$

Full-length APP has been found to interact with collagen, laminin and heparin which all mediate cell adhesion [72-74]. Furthermore, APP, APLP-1 and APLP-2 have been shown to form dimers and multimers both *in vivo* and *in vitro* and interact both at the cell surface and intracellularly suggesting a role for this self-association in cell adhesion [75].

APP has also been strongly implicated in trophic functions with APP-deficient neurons exhibiting decreased survival, axonal branching and minor process production [76]. The trophic role of APP is thought to be related, at least in part, to the generation of sAPP $\alpha$  which has been found to mediate synaptic growth via a process involving the 'RERMS' motif within the fragment [52]. Clearly, APP has a role to play in brain development and function as, despite being viable and fertile, APP knockout mice show a 10% decrease in brain weight and exhibit significant hippocampal abnormalities along with spatiotemporal learning consistent with impaired long term potentiation [77]. The lack of a more severe phenotype exhibited by APP knockout mice is thought to be due in part to a compensatory role played by APLP-1 and/or APLP-2. Indeed, triple knockout (APP, APLP-1 and APLP-2) mice die shortly after birth and show significant synaptic abnormalities [78]. Synaptic terminals in APP+APLP2 knockout mice are incorrectly juxtaposed suggesting that the APP gene family is essential in synaptogenesis [77].

sAPP $\alpha$ , in particular, is thought to exhibit a neuroprotective function and recent findings that this fragment reduces expression of CDK-5 (a kinase that

induces neurodegeneration and indirectly increases amyloidogenic processing of APP) provide a potential mechanism for its neuroprotective properties [79].

#### 1.4.2. AICD

Both the AICD and Notch intracellular domains co-localise to nuclear spots and form transcription complexes with Fe65 and Tip60 [80]. In fact, both fragments can influence the expression of a range of proteins (Table 1.3). Of particular relevance to AD is the fact that AICD expression has been linked to both increased APP mRNA levels and decreased APP half-life suggesting that, whilst the fragment enhances APP transcription, it may also promote the transcription of genes regulating the turnover of the APP protein [81].

**Table 1.2. AICD target genes.** Adapted from Pardossi-Picquard & Checler [54].

<b>AICD target gene</b>	<b>Function</b>	<b>Up- or down-regulation</b>
<b>KAI1/CD82</b> <b>GSK3<math>\beta</math></b>	<ul style="list-style-type: none"> <li>• Metastasis suppressor, apoptosis</li> <li>• Cell cycle regulation, proliferation, apoptosis</li> </ul>	Up
<b>APP</b> <b>BACE</b> <b>Neprilysin</b>	<ul style="list-style-type: none"> <li>• Cell adhesion, synaptogenesis, neurite outgrowth</li> <li>• APP cleavage</li> <li>• A<math>\beta</math>-degrading enzyme</li> </ul>	Up Up Up
<b><math>\alpha</math>2 actin</b> <b>Transgelin</b>	<ul style="list-style-type: none"> <li>• Organisation and dynamics of actin cytoskeleton</li> </ul>	Up
<b>EFGR</b> <b>LRP1</b>	<ul style="list-style-type: none"> <li>• Cell cycle proliferation, differentiation, survival</li> <li>• Endocytosis and signalling, transport of ApoE</li> </ul>	Down

### **1.4.3. A $\beta$ -peptides**

In contrast to the neurotoxic effects of A $\beta$ -peptides associated with AD, picomolar concentrations of A $\beta$ 42 significantly improved both long-term potentiation and multiple hippocampal-mediated memory functions in mice transfused with the peptide [82]. This supports a physiological role for lower A $\beta$  concentrations in long-term potentiation that is perhaps lost in AD.

## **1.5. Copper, Alzheimer's disease and APP**

Copper is a trace element essential to human life. It serves as an allosteric regulator or catalytic cofactor in many metalloenzymes including cytochrome c oxidase, lysyl oxidase, ceruloplasmin, superoxide dismutase and catechol oxidase. These enzymes are critical in the normal function of bodily processes such as mitochondrial respiration, antioxidant defence, biometal transport and connective tissue formation. Copper further acts as a transcriptional regulator for metal responsive Ace1, Amt1 and Mac1 genes, which control intracellular accumulation of transition metals [83].

Humans consume 0.6-1.6 mg of copper a day which originates from pulses, nuts, grains and shellfish [84]. However, high concentrations of copper are extremely toxic due to the ability of the metal to generate ROS via Fenton's chemistry, contributing to oxidative stress and the oxidation of lipids, nucleic acids and proteins [85]. Therefore, humans have developed complex copper homeostatic mechanisms.

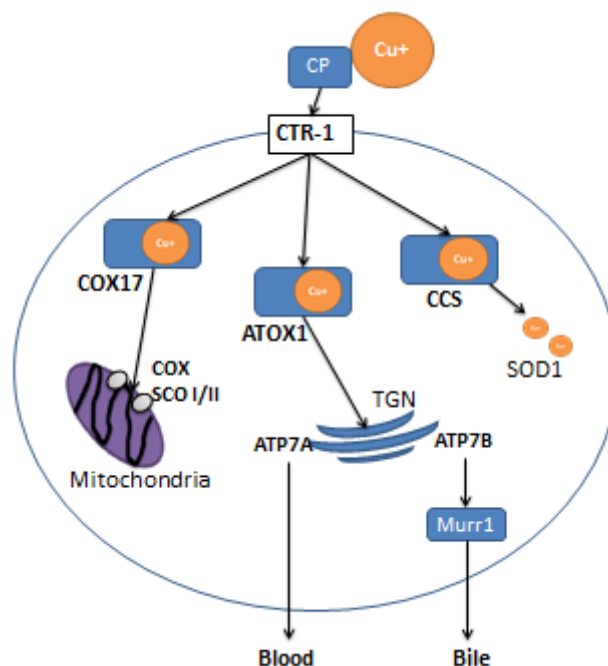


**Figure 1.4. Simplified uptake of copper into cells.** The majority of circulating copper is bound to Ceruloplasmin (CP). Copper enters the cell via the transporter CTR-1 and binds to the chaperones COX17, ATOX1 and CCS. COX17 facilitates the transport of copper to the mitochondria, where it interacts with the SCO proteins to transport copper to cytochrome-c oxidase (COX), which is essential for normal mitochondrial function. CCS transfers the copper to superoxide dismutase (SOD1) which is an antioxidant. ATOX1 transports copper to the ATP7A/ATP7B in the Golgi. ATP7A transports copper back into the blood whilst ATP7B transports copper to the bile via Murr1. Adapted from Lutsenko *et al.* [4]

In mammals, copper uptake occurs in the enterocytes of the digestive tract and the liver via the copper plasma membrane transporter 1 (CTR1). Chaperone proteins transport copper to the copper transporters ATP7A (enterocytes) and ATP7B (liver) where copper is released into the portal vein or blood stream for uptake by the body [83]. Excess copper is re-transported into the intestinal epithelium or into bile for

excretion (Fig. 1.4). The majority of circulating copper is bound to ceruloplasmin (approximately 65% of the total copper) or albumin (approximately 18%) [86, 87]. Copper uptake across the blood-brain-barrier is reportedly mediated by ATP7A transporters [85].

The importance of copper homeostasis is demonstrated through diseases related to defective copper transport such as Menkes disease in which a mutation within the ATP7A transporter impairs the absorption of copper from the intestinal tract and its transport into the blood stream [88]. This manifests as extreme copper deficiency with associated neurodegeneration and connective tissue abnormalities. Similarly, Wilson's disease, a disorder of the ATP7B transporter, results in the impaired excretion of copper from the liver causing liver cirrhosis and elevated free copper concentrations in the blood leading to ROS generation [88].

### **1.5.1. Copper and Alzheimer's disease**

Pajonk *et al.* [89] demonstrated that cognitive test scores in AD patients negatively correlated with plasma copper concentrations indicating that copper deficiency may be linked to the disease. Conversely, Smorgon *et al.* [90] demonstrated a significantly higher serum copper concentration in AD patients compared to age-matched controls. Although research of this type has been consistently disparate, a meta-analysis study did find a small but significant increase in copper concentrations in the blood and cerebrospinal fluid of AD patients compared with controls [91].

In terms of brain tissue, significant decreases in copper concentration have been demonstrated in the amygdala and hippocampus of AD patients with lower, but

not significantly different, concentrations in other areas of the brain [92]. In apparent contrast, Religa *et al.* [93] found a higher copper concentration specifically in the neuropil of the amygdala suggesting that copper was transported out of the cells more effectively in AD patients. Collectively, these studies, although partially contradictory, nonetheless demonstrate a complex inter-relationship between copper homeostasis and AD.

### **1.5.2. Copper and APP expression**

Copper has been implicated in the regulation of APP transcription, translation and proteolysis in multiple studies. Cater *et al.* [94] demonstrated a reduction of *APP* mRNA expression under copper deficient conditions in fibroblasts expressing mutant ATP7A / ATP7B transporters. However, the authors showed that APP protein expression remained stable suggesting that copper deficiency enhanced the translation efficiency of *APP* mRNA. Similarly, Armendariz *et al.* [95] demonstrated a 2.2-fold increase in *APP* expression through chronic copper dosing of primary neurons. Bellingham *et al.* [96] demonstrated an 80% reduction in *APP* promoter activity when the -490 to +104 region of the *APP* promoter was deleted. The same study also found that copper levels positively correlate with APP levels, supporting findings by Armendariz *et al.* [95]. Taken together, these studies promote the existence of a copper responsive element in the -490 to +104 region of the APP promoter that increases APP transcription in increased copper concentrations.

*In vivo* studies in APP knockout mice show a 40% increase in copper concentrations in the cerebral cortex compared to WT mice [97]. The authors proposed that low antioxidant defence in neurons results in the tight regulation of copper by APP [97].

### **1.5.3. Copper and APP proteolysis / trafficking**

Copper has been shown to decrease A $\beta$  generation and enhance the non-amyloidogenic production of sAPP $\alpha$  at metal concentrations as low as 10  $\mu$ M [98]. Similarly, Cater *et al.* [94] showed a significant switch from sAPP $\alpha$  to sAPP $\beta$  secretion in a copper-deficient cell model.

In terms of APP trafficking, studies using a C-terminally fluorescent-tagged form of APP demonstrated a 2-fold increase in cell surface levels of the protein following the treatment of SH-SY5Y cells with copper [99]. The enhanced cell surface levels of APP were accompanied by a reduction in Golgi-associated protein and its increased exocytosis.

Lipid rafts have also been linked to copper and APP trafficking/proteolysis. Hung *et al.* [100] found that increased copper levels correlated inversely with  $\gamma$ -secretase localisation to lipid rafts and that copper promoted the cell surface localisation of APP, which increases non-amyloidogenic APP processing. The same study found that copper levels exhibited an inverse relationship with lipid raft copper concentrations. This suggests that copper deficiency both increases amyloidogenic processing and co-localises A $\beta$  to copper in lipid rafts, facilitating the formation of pro-oxidant A $\beta$ :Cu (II) complexes that contribute to oxidative stress [100].

### **1.5.4. APP and the regulation of copper toxicity**

The fact that APP is known to reduce Cu (II) to Cu (I) [101] has led to much research investigating whether the protein can regulate copper-induced toxicity in cells. The enhanced expression of APP in cells expressing mutant ATP7A / ATP7B transporters (which exhibit a 5-fold increase in intracellular copper levels) indicates that the former protein is indeed involved in the cellular response to elevated copper

[95]. The cytoprotective role of APP against copper is further supported by the experiments of Cerpa *et al.* [102] which demonstrated that peptides mimicking the E1 copper binding domain of APP protected mice against the spatial memory impairment, neuronal cell loss and astrogliosis caused by the injection of copper chloride into their brains. No such protection was observed when a similar peptide lacking crucial copper-binding histidine residues was employed.

However, conversely, other studies suggest that APP actually facilitates copper-induced toxicity. White *et al.* [35] demonstrated that neurons from APP knockout mice were more resistant to copper toxicity than their counterparts expressing normal APP levels. The same group also showed that, when the APP knockout neurons were treated with a peptide mimicking the APP E1 copper binding domain, copper-induced toxicity was increased. White *et al.* [103] also demonstrated a peroxidising capability of full-length APP that is also present in APLP2 and non-human orthologues.

#### **1.5.5. APP and A $\beta$ aggregation / clearance**

Although high levels of copper (400  $\mu\text{M}$ ) are present in senile plaques [104] it is unclear whether it is metal binding that promotes A $\beta$  aggregation or whether the A $\beta$  aggregates, once formed, sequester metal. The former possibility is supported by evidence that A $\beta$  fibrillisation is accelerated by trace concentrations of both copper and zinc ( $\leq 0.8 \mu\text{M}$ ); an effect that was negated in the presence of a metal chelator [105]. Conversely, Innocenti *et al.* [106] used atomic force microscopy to demonstrate that low copper and zinc concentrations (0.1-1  $\mu\text{M}$ ) stabilized non-fibrillar A $\beta$  oligomers. Similarly, Curtain *et al.* [107] showed that copper promoted a change in

A $\beta$  conformation from  $\beta$ -sheet to  $\alpha$ -helix thereby supporting oligomer rather than fibril formation.

The second possibility, i.e. that A $\beta$  aggregates sequester copper, is supported by the observation that A $\beta$  aggregates bind Cu(II) with an affinity two orders of magnitude higher than that observed for A $\beta$  monomers facilitating the sequestration of the metal from albumin [108]. This high affinity was attributed to a co-ordination sphere of a total of three histidine residues contributed by two adjacent A $\beta$  peptides.

Recently, Singh *et al.* [109] suggested that copper accumulation in the brain might impair the clearance of A $\beta$  across the blood-brain-barrier by the low density lipoprotein receptor-related protein 1 (LRP1). The authors showed that chronic copper dosing in young mice enhanced A $\beta$  levels in the brain with a concomitant decrease in levels of LRP-1. Furthermore, LRP-1 deficient mice exhibited increased brain A $\beta$  levels and neuroinflammation.

#### **1.5.6. Copper and the mediation of A $\beta$ neurotoxicity**

Both A $\beta$ 40 and A $\beta$ 42 are known to stimulate ROS production, lipid peroxidation and DNA oxidation (reviewed in [110]), and it is possible that copper binding to A $\beta$  mediates this process. A $\beta$  peptides bind to Cu(II) with a stoichiometry of 1:1 [111]. Huang *et al.* [112] found that A $\beta$  binds Cu (II) and reduces it to Cu (I), generating the potent oxidiser hydrogen peroxide. The reducing potential of the A $\beta$  molecule was subject to its length, with A $\beta$ 42 exhibiting the greatest reducing potential. In their following paper, Huang *et al.* [113] demonstrated that the reduction of Cu (II) by A $\beta$  was directly responsible for the generation of hydrogen peroxide through an electron transfer chain that facilitated the reduction of oxygen. Further

studies have confirmed the ability of A $\beta$  to generate hydrogen peroxide, which consequentially generates hydroxyl radicals *in vitro* (reviewed in [114]). Taken together, these studies confirmed that A $\beta$ :Cu complexes generate ROS that may induce the neurotoxicity observed in AD.

#### **1.5.7. APP as a copper binding protein**

In addition to the binding of copper to A $\beta$  (it is not clear whether the metal binds this region in the full-length APP protein) APP possesses at least two other high affinity copper binding domains within the extracellular E1 and E2 domains.

##### ***1.5.7.1. The E1 copper binding domain***

The E1 CuBD is located between amino acids 28 and 129 of APP [1]. The structure of the domain has been solved by nuclear magnetic resonance spectroscopy and X-ray crystallography and comprises an  $\alpha$ -helix packed against three anti-parallel  $\beta$ -strands [115]. The putative binding site consist of histidines 147 and 151, tyrosine 168 and an axial water and equatorial water molecule which together form a tetrahedrally distorted square planar geometry when bound [115]. This binding site is referred to as a Type 2 non-blue Cu centre due the involvement of histidine nitrogen ligands and oxygen ligands. Methionine 170 is thought to act as an electron donor in the reduction of Cu(II) to Cu(I), and the surface localisation and Type 2 centre further support a role for this CuBD in the redox cycling of Cu(II) to Cu(I) [116].

A study examining the potential role of the E1 CuBD in APP cell biology demonstrated decreased APP maturation, ER to Golgi trafficking and folding when histidine residues 149 and 151 were mutated to asparagine [117]. The relevance of the

replacement of histidine to asparagine is biologically debateable as the latter is rarely found in helical structures [118] (in which the copper co-ordinating histidine residues of the E1 CuBD are located) and is likely to disrupt such secondary structure.

#### **1.5.7.2. The E2 copper binding domain**

The E2 copper binding domain of *APP* is located between residues 295 and 500 of the ectodomain (*APP*<sub>695</sub> numbering) [119]. X-ray crystallography of the *APP* E2 domain demonstrated a structure consisting of four  $\alpha$ -helices surrounding a hydrophobic core. Using cadmium ions as markers of potential metal binding sites, Dahms *et al.* [119] identified a well-conserved potential copper binding site comprised of four histidine residues at positions 313, 382, 432 and 436 (*APP*<sub>695</sub> numbering) from the  $\alpha$ -B,  $\alpha$ -C and  $\alpha$ -D helices which coordinate around a ‘tetrahedrally distorted square planar’ structure when bound. The authors demonstrated an upper limit dissociation constant of  $K_d \leq 13$  nM for copper binding to this site and demonstrated that copper (or zinc) binding to the *APP* E2 CuBD caused a significant conformational change in domain structure. Furthermore, limited proteolysis experiments demonstrated that the structure of the full-length *APP* protein was more resistant to degradation when bound to copper within the E2 domain.

### **1.6. Aims of the current project**

Although copper is now known to bind to the E2 domain of *APP*, no studies have examined the effects of this binding on the cell biology of the protein. In the current study, histidine to alanine mutant constructs (within the E2 CuBD) will be used in order to study any potential effects of metal binding within this domain on the following aspects of *APP* cell biology:

- (i) APP expression and proteolysis.
- (ii) The effect of E2 copper binding on copper-induced cytotoxicity.
- (iii) The effect of E2 copper binding on the subcellular localisation of APP.

## **2. Materials and Methods**

## **2.1. Materials**

All tissue culture reagents were purchased from Lonza (Basel, Switzerland) and all other reagents, unless otherwise stated, were purchased from Sigma-Aldrich (Poole, U.K.). pIRESHyg mammalian expression vector was from Invitrogen (Paisley, U.K.). The APP<sub>695</sub>-pIRESHyg vector has been described previously [120] and was used, by Epoch Biolabs (Texas, U.S.A.) as a template to generate histidine to alanine APP substitution mutants as described in the Results section.

Anti-APP C-terminal polyclonal antibody, anti-actin monoclonal antibody and secondary peroxidase-conjugated antibodies were from Sigma-Aldrich (Poole, U.K.). Anti-APP 6E10 monoclonal antibody was from Covance (Princeton, U.S.A.) and the anti-APP polyclonal antibody used in the immunofluorescence studies was from Abcam (Cambridge, UK). The anti-sAPP $\beta$  1A9 monoclonal antibody was kindly provided by Prof. Nigel Hooper (Manchester, U.K.).

## **2.2. Methods**

### **2.2.1. Bacterial transformation**

DNA (approximately 1  $\mu$ g) was incubated with 20  $\mu$ l of XL-1 Blue competent *E. Coli* (Agilent Technologies, Stockport, UK) for 20 min at 4°C. The cells were then heat shocked at 42°C for 45 sec and then incubated at 4 °C for an additional 2 min.

### **2.2.2. Preparation of agar plates and bacterial culture**

Liquid broth (LB) was prepared by dissolving 10 g of low salt granulated broth (Melford, Ipswich, U.K.) in 500 ml of distilled water. Agar (Melford, Ipswich, U.K.) (5 g) was added to the LB and the solution was then autoclaved for 30 min. After

cooling to 40 °C, ampicillin stock (100 mg ml<sup>-1</sup>) was added to the agar to a final concentration of 50 µg ml<sup>-1</sup>. Plates were then poured, allowed to cool and stored inverted at 4 °C until use.

Transformed cells (10 µl) were streaked onto an agar plate and cultured overnight at 37 °C. Colonies were then stabbed and transferred to 50 ml of LB containing 50 µg ml<sup>-1</sup> ampicillin that had been autoclaved previously in conical flasks. These 'midi-cultures' were grown at 37 °C on an orbital shaker overnight.

### **2.2.3. DNA purification**

The contents of a single midi-culture (see section 2.2.2. above) were centrifuged at 6000 g for 15 min and DNA was purified from the pellets using the Qiagen® Plasmid Midi Purification Kit according to the manufacturer's protocol. DNA concentrations were determined using the NanoDrop®2000 spectrophotometer, and the DNA was stored at -20 °C.

### **2.2.4. Ethanol precipitation of DNA**

DNA prepared as described above was combined with 1/10 volume of 3 M sodium acetate (pH 5.2) and two volumes of cold absolute ethanol. This mixture was then incubated at -20 °C for 1 h prior to centrifuging for 20 min at 11,600 g at 4 °C. The supernatant was removed and replaced with 300 µl of 80% (v/v) ethanol without disturbing the pellet. The sample was then centrifuged once more under the same conditions for 5 min. The supernatant was removed again and the DNA was resuspended in filter-sterilized distilled water (30 µl) under aseptic conditions.

### **2.2.5. Mammalian cell culture**

Human neuroblastoma, SH-SY5Y, and human embryonic kidney (HEK) cells were cultured in Dulbecco's Modified Eagle's medium (DMEM) high glucose with L-glutamine, supplemented with 10%, (w/v) foetal bovine serum, penicillin (100 units ml<sup>-1</sup>) and streptomycin (100 µg ml<sup>-1</sup>). The cells were grown in 5% CO<sub>2</sub>. Once confluent, cells were washed with 2 ml trypsin before replacing with a fresh 2 ml and incubating at room temperature until the cells were released from the flask base. The trypsin was then deactivated by the addition of complete growth medium (10 ml). Cells were then pelleted by centrifugation for 3 min at 1500 g and resuspended in the appropriate volume of complete growth medium prior to seeding at the required density.

For long term storage, cell pellets were resuspended in 1 ml complete growth medium containing 10% (v/v) dimethyl sulfoxide (DMSO). The cells were transferred to cryovials (Corning, New York, U.S.A.) and snap frozen in liquid nitrogen.

### **2.2.6. Transient transfection of HEK cells**

The following procedures were all performed under aseptic conditions. HEK cells were grown to 80% confluence at which point the growth medium was removed and cells were washed *in situ* with 10 ml UltraMEM™. A fresh 10 ml of UltraMEM™ was then added to the cells and they were incubated for 30 min at 37 °C in 5% CO<sub>2</sub>. During this incubation period, 8 µg of ethanol precipitated DNA (see section 2.2.4 above) was diluted to 500 µl using UltraMEM™. A second solution was also made consisting of 20 µl Lipofectamine®2000 (Life™ Technologies, Carlsbad, U.S.A.) and 480µl UltraMEM™. These two solutions were incubated for 5 min at room temperature, combined and then incubated for a further 20 min at the same

temperature. During this time the medium was removed from the cells and replaced with a fresh 2 ml of UltraMEM™. The DNA: Lipofectamine®2000 complexes were then added drop-wise to the cells with constant gentle swirling. The cells were returned to the growth incubator for 5 h after which 5 ml of DMEM containing 30% (v/v) FBS (no penicillin or streptomycin) was added to each flask. The cells were then cultured for an additional 24 h followed by the removal of spent medium and its replacement with 10 ml of complete growth medium. Following an additional 24 h incubation the transfectants were ready to use for experiments.

#### **2.2.7. Stable transfection of HEK and SH-SY5Y cells**

For stable transfections, 8 µg (Lipofectamine® protocol) or 20 µg (electroporation protocol) of DNA was linearized in a solution consisting of DNA, Ahd1 restriction enzyme (3 µl), 10 x restriction buffer (5 µl), BSA (1 mg ml<sup>-1</sup>) and distilled water to make up to 50 µl. After overnight incubation at 37 °C, the DNA was ethanol precipitated as described in section 2.2.4.

HEK cells were then stably transfected using the lipofectamine method described above (section 2.2.6.). Stable transfectants were then selected by culturing the cells in the presence of hygromycin B (150 µg ml<sup>-1</sup>) (Invitrogen, Paisley, U.K.).

SH-SY5Y cells were stably transfected by electroporation. Cells were grown to 60% confluence before trypsinising as described in section 2.2.5. The cell pellets were resuspended in 800 µl UltraMEM™ and transferred to a 2 mm mammalian transfection cuvette (Bio-Rad, Hemel Hempstead, UK) along with the ethanol precipitated DNA in a volume of 30 µl. Following thorough mixing by repeat pipetting, the cells were subjected to electroporation (square wave programme, 120 V,

25 ms) using a Gene Pulser Xcel™ electroporator (Bio-Rad, Hemel Hempstead, U.K.). The cuvette was then transferred to ice for 10 min before mixing the contents of the cuvette thoroughly with 5 ml complete growth medium. The cells were then transferred to 10 ml complete growth medium in culture flasks and grown to confluence before selecting stable transfectants using hygromycin B as described above.

#### **2.2.8. Preparation of cell lysates and conditioned medium samples**

Following cell treatments, conditioned medium was removed and centrifuged for 5 min at 1500 g. The supernatant was then transferred to an Amicon Ultra-15 Centrifugal Filter Unit (Millipore, Watford, U.K.) which, prior to use, had been equilibrated in distilled water (10 ml) for 10 min. The supernatant was centrifuged at 3000 g (4 °C) until the volume was reduced to approximately 400 µl. Protein concentrations were determined (see section 2.2.9) and the samples were equalized in terms of protein by diluting with distilled water before freezing at -20 °C pending further use.

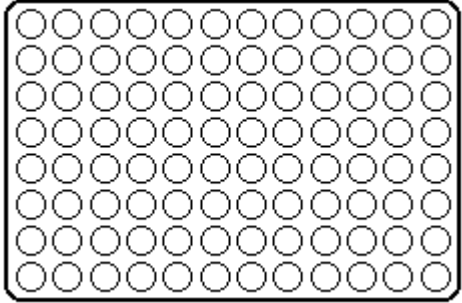
For the preparation of cell lysates, the cells were washed *in situ* using 20 ml of phosphate-buffered saline (PBS; 1.5 M NaCl, 20 mM NaH<sub>2</sub>PO<sub>4</sub>, 200 mM Na<sub>2</sub>HPO<sub>4</sub> made up in distilled water, pH 7.4). The cells were then scraped from the flasks into a fresh 10 ml PBS and transferred to a Falcon tube. Flasks were rinsed with an additional 5 ml PBS which was transferred to the same Falcon tube. Cells were pelleted by centrifugation at 1500 g (3 min) before removing the supernatant and resuspending the cells in 2 ml of lysis buffer (0.1 M Tris, 0.15 M NaCl, 1% (v/v) Triton X-100, 0.1% (v/v) Nonidet P-40, pH 7.4) containing 10 mM 1,10-phenanthroline. After resuspension, the cells were sonicated for 30 sec using a probe

sonicator (MSE, Crawley, U.K.) and the lysates were transferred to Eppendorf tubes and centrifuged at 11,600 g for 10 min. The supernatants were then assayed for protein (see section 2.2.9) and the samples were equalized in terms of protein by diluting with lysis buffer. The final lysate preparations were then frozen at -20 °C pending further analysis.

### **2.2.9. Bicinchoninic acid (BCA) protein assay**

The BCA protein assay was performed using bovine serum albumin (BSA) standards made up in distilled water and loaded (10 µl) into a 96-well microtitre plate as shown in Table 2.1. Samples of cell lysates (3 µl) or concentrated conditioned medium (5 µl) were loaded in duplicate starting at row B on the plate. Assay reagent (a 50:1 (v/v) ratio of BCA stock solution (Pierce, Illinois, U.S.A.) and 4% (w/v) CuSO<sub>4</sub> · 5H<sub>2</sub>O) was then added (200 µl) to all wells (standards and samples) and the plate was incubated for 30 min at 37 °C. Absorbances of the samples were read at 570 nm using a PerkinElmer VIKTOR™ plate reader. A BSA standard curve was generated and the protein concentrations of samples were extrapolated from this graph.

**Table 2.1. BSA standards and their loading in 96 well plates.**

Standard	[BSA] (mg/ml)	Wells loaded
		<div style="display: flex; justify-content: space-around; font-size: small;"> <span>1</span><span>2</span><span>3</span><span>4</span><span>5</span><span>6</span><span>7</span><span>8</span><span>9</span><span>10</span><span>11</span><span>12</span> </div> 
A	0.2	A1 and A2
B	0.4	A3 and A4
C	0.6	A5 and A6
D	0.8	A7 and A8
E	1.0	A9 and A10
F	0	A11 and A12

### **2.2.10. Sodium dodecylsulphate-polyacrylamide gel electrophoresis (SDS-PAGE)**

Protein samples (20-40  $\mu$ l) were denatured by the addition of 0.5 volumes of dissociation buffer (10% (w/v) SDS, 80 mM dithiothreitol, 20% (v/v) glycerol, 140 mM Tris-HCl pH 6.8, few drops of 0.05% (w/v) bromophenol blue) and subsequent boiling for 3 min. Molecular weight standards (GE Healthcare, Buckinghamshire, U.K.) were prepared in the same way, without the subsequent boiling.

Equal volumes of protein-equalized samples were then resolved on 5-15% or 7-17% polyacrylamide gradient gels. The stacking and resolving gels were prepared according to the recipes detailed in Table 2.2.

**Table 2.2. SDS-PAGE resolving and stacking gel constituents.**

<i>Reagent</i>	<i>Resolving gel solutions</i>				<i>Stacking gel</i>
	<i>17%</i>	<i>7%</i>	<i>15%</i>	<i>5%</i>	
Sucrose	0.37 g	-	0.33 g	-	-
Tris/HCl pH 8.8	1.39 ml	1.39 ml	1.39 ml	1.39 ml	-
Tris/HCl pH 6.8					0.63 ml
30% acrylamide, 0.8% Bis (Universal Biologicals, Cambridge, U.K.)	2.1 ml	0.88 ml	1.9 ml	0.63 ml	0.5 ml
Distilled water	-	1.36 ml	0.22 ml	1.64 ml	3.83 ml
1.5% (w/v) ammonium persulphate	0.22 ml	0.1 ml	0.2 ml	71 $\mu$ l	0.25 ml
10% (w/v) SDS	37 $\mu$ l	37 $\mu$ l	37 $\mu$ l	37 $\mu$ l	50 $\mu$ l
N,N,N',N'- Tetramethylethylenediamine (TEMED)	3 $\mu$ l	3 $\mu$ l	3 $\mu$ l	3 $\mu$ l	5 $\mu$ l

Prior to the addition of TEMED, the solution was vortexed briefly and poured using a gradient mixture with a peristaltic pump. Once poured water-saturated isobutanol was pipetted over the top layer of the gel to eliminate any air bubbles and provide a marker of when the gel had set, and the gel was left for at least 15 minutes. Once set the water-saturated isobutanol was poured off the gel, washed with ddH<sub>2</sub>O, and the

stacking gel was pipetted onto the gel following the above protocol. This was left to set for a further 15 minutes.

Protein samples were denatured for 3 minutes at 95°C to stabilise the proteins for electrophoresis. Disassociation buffer was added to the samples at half the volume of the sample. Gels were loaded onto the electrophoresis tank and filled with running buffer (1x Tris/glycine/SDS, GeneFlow Ltd, Fradley, UK). Pre-diluted protein ladder (GE Healthcare, UK) was also diluted with denaturing buffer at the same concentration as the samples and 20µl added to the initial well, followed by 20µl of each sample. Gels were run at 300V in running buffer (0.25 M Tris, 1.92 M glycine, 1% (w/v) SDS, diluted with distilled water from a 10 x stock) (GeneFlow Ltd, Fradley, U.K.) at 35 mA per single gel constant current until the dye front reached the bottom of the gel.

#### **2.2.11. Western blotting**

Following SDS-PAGE, resolving gels were transferred to Immobilon-P PVDF (polyvinylidene fluoride) membranes (Millipore, Massachusetts, U.S.A.) in Towbin buffer (800 ml methanol, 20 mM Tris, 150 mM glycine, made up to 4 L with distilled water) at 115 V for 1 h.

Membranes were then washed with PBS for 5 min and blocked for 1 h in 5% (w/v) Marvel milk powder in PBS + 0.1% (v/v) TWEEN-20 (PBS-TWEEN). The membranes were then washed once more for 5 min in PBS and incubated overnight with shaking (4°C) in primary antibody at the dilutions described in Table 2.3 made up in PBS-TWEEN + 2% (w/v) BSA. The following morning, the membranes were washed for 1 x 1 min and 2 x 15 min in PBS-TWEEN. The appropriate secondary

antibody (see Table 2.3.) was then incubated with the membranes for a further 1 h at room temperature before washing them in PBS lacking Tween (1 x 1 min, 2 x 15 min). ECL Western blotting substrate (ThermoFisher Scientific, Cramlington, UK.) was added to the membrane for approximately 2 min before developing the blot by exposure to X-ray film (ThermoFisher Scientific, Cramlington, UK.). Developed blots were stained for 2 min in amido black (40% (v/v) methanol, 10% (v/v) acetic acid 0.01% (w/v) amido black in distilled water), to visualise bound proteins.

### **2.2.12. Stripping and re-probing immunoblots for anti-actin**

Membranes were incubated at 50 °C for 30 min in stripping buffer (100 mM  $\beta$ -mercaptoethanol, 2% (w/v) SDS, 62.5 mM dd H<sub>2</sub>O, pH6.7) to remove bound proteins. Following two 10 min washes in PBS-TWEEN, the immunoblots were then blocked and processed as described previously (section 2.2.11).

**Table 2.3. Antibody dilutions for Western blotting.**

<b>Antibody</b>	<b>Dilution</b>
Anti-APP C-terminal	1:7500
Anti-APP 6E10	1:2500
Anti-sAPP $\beta$ 1A9	1:3000
Anti-actin	1:5000
Anti-Mouse IgG–Peroxidase Antibody raised in rabbit	1:4000
Anti-Rabbit IgG–Peroxidase antibody raised in goat	1:4000

### **2.2.13. Copper toxicity assays**

Cells were grown in T75 cm<sup>2</sup> flasks until they reached ultra-confluency to ensure subsequent seeding at the same densities. Following trypsinization, the cell pellets were resuspended in complete growth medium (10 ml). Cells (100-150 µl according to cell line) were then seeded in 1 ml of DMEM in the wells of a 24-well plate. Cells were grown to confluency before removing the spent growth medium and washing the cells with UltraMEM™ (1 ml). The UltraMEM™ was then replaced with a fresh 1 ml of the same medium containing the desired final concentrations of copper (achieved by adding the appropriate volume of a filter-sterilized 10 mM CuSO<sub>4</sub> solution or 100mM CuCl<sub>2</sub>:glycine complex stock solution ). The cells were then cultured for 48 h after which the medium was removed and the cells were washed with UltraMEM™ (1 ml) before replacing this with a fresh 500 µl of the same medium. CellTiter 96® Aqueous One Cell proliferation Assay solution (methanethiosulfonate; MTS) (100 µl) was then added to each well and the plate was incubated at 37°C until a colour change was observed. The contents of each well were transferred to a 96 well plate to read the absorbance (490 nm).

### **2.2.15. Immunofluorescence**

Cells were grown to 80% confluence on coverslips placed in the wells of a cell culture plate. The coverslips were then transferred to a fresh culture plate and washed (2 x 5 min) in PBS. The cells were then fixed by the addition of either absolute methanol or 3% (w/v) paraformaldehyde, pH 7.4 and subsequent incubation at room temperature for 10 min. Each coverslip was then incubated in immunofluorescence (IF) buffer (0.025% (w/v) SDS, 0.1% (v/v) Triton, 1% (w/v) BSA in PBS) for 1 h at room temperature. Primary anti-APP antibody (ab15272) (Abcam, Cambridge, UK) was then diluted at 1:100 in IF buffer prior to centrifugation for 5 min at 11,600 g. The antibody supernatant (300 µl) was then added to the cells (after removing the last

IF buffer wash) and the plate was wrapped in tin foil and incubated overnight on an orbital shaker at 4 °C. The following morning, the cells were washed (1 x 1 min and 2 x 15 min) in PBS-TWEEN. Anti-Rabbit IgG-FITC antibody (Sigma Aldrich, Poole, UK) was diluted to 1:300 in IF buffer and centrifuged as per the primary antibody before adding 300 µl to each coverslip (after removal of the final PBS-TWEEN wash). After a 1 h incubation on the orbital shaker at room temperature, the secondary antibody was removed and the coverslips were washed in 200 µl of 4',6-diamidino-2-phenylindole (DAPI) in PBS (1:1000) for 5 min in order to optimise nuclear staining. Final washes of the coverslips for 1 x 1 min and 2 x 15 min were performed in PBS. The coverslips were then removed from the wells of the plate and placed face down onto slides with a drop of VECTASHIELD® with DAPI in order to prevent cell bleaching. Cells were visualised by confocal microscopy (Zeiss, Cambridge, UK) using 405 nm and 561 nm excitation wavelengths.

#### **2.2.16. Statistical analysis**

Statistical analysis was performed using the Student's t-test. Differences were recognised as significant with a P-value of  $\leq 0.05$  (\*) or  $\leq 0.005$  (\*\*). For all results n=3 unless otherwise stated.

## **3. Results**

### **3.0 Introduction**

As already discussed, Dahms *et al.* [119], identified a copper binding site within the E2 domain of APP. The authors demonstrated that the co-ordination of copper within this site involved four histidine residues at positions 313, 382, 432 and 436 (APP<sub>695</sub> numbering). However, the same group did not examine the effect of these residues on the cell biology of APP; something that clearly has relevance to AD pathogenesis. Therefore, in the current study, APP<sub>695</sub> mutants containing histidine to alanine substitutions within the E2 CuBD have been employed in order to study the effects of this domain on the expression, proteolysis and localisation of APP. The possible role of the E2 CuBD in regulating cytotoxicity has also been examined.

Five APP<sub>695</sub> mutant constructs were employed in which the APP coding DNA was inserted into the mammalian expression vector pIRESHyg (Invitrogen, Paisley, U.K.). These constructs consisted of single histidine to alanine substitutions at positions 313, 382, 432 or 436 named APP-E2 CuBD H313A, APP-E2 CuBD H382A, APP-E2 CuBD H432A and APP-E2 CuBD H436A. A fifth construct contained all four of these substitutions, APP-E2 CuBD AAAA (Fig. 3.1.)

#### **3.1. Transient expression and proteolysis of constructs in HEK cells**

In order to validate the mutant APP constructs they were initially transiently expressed in HEK cells. This was a relatively quick method that did not necessitate the weeks of antibiotic selection required for the generation of stable transfectants. HEK cells were transiently transfected with either pIRESHyg vector alone (mock), Wild-type APP (Wt- APP) or the five histidine to alanine constructs (see Materials and Methods). The cells were then

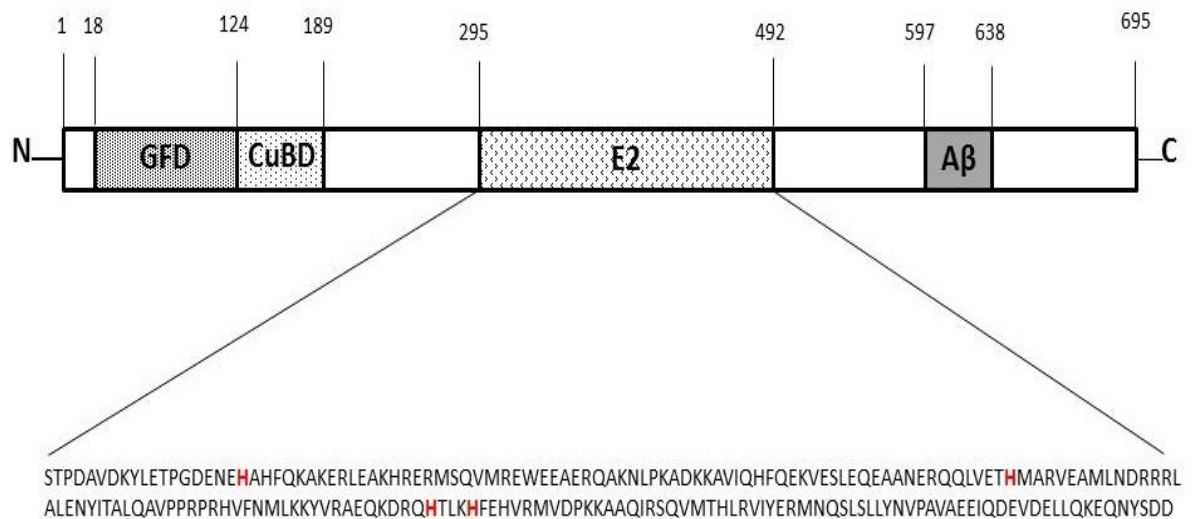


**Figure 3.1. A schematic diagram of APP<sub>695</sub> showing the location of the residues mutated in the current study.. GFD; Growth factor-like domain, CuBD; E1 copper binding domain**

incubated in UltraMEM™ for 24 h and cell lysates and conditioned medium samples were prepared (see Materials and Methods).

Initially the cell lysates were immunoblotted with the anti-APP C-terminal antibody. The results (Fig. 3.2A.) clearly show that both Wt-APP and the E2 CuBD mutants were highly over-expressed relative to the endogenous protein in mock-transfected cells. Furthermore, excluding the APP-E2 CuBD H436A mutant, there were no significant differences between the expression of any of the E2 CuBD mutants and the over-expressed wild-type protein. HEK cells overexpressing the H436A mutant expressed approximately 1.4-fold more APP relative to the Wt-APP over-expressing cells. The blots were then stripped and re-probed with the anti-actin antibody in order to confirm equal protein loading which was shown to be consistent between samples (Fig. 3.2B.).

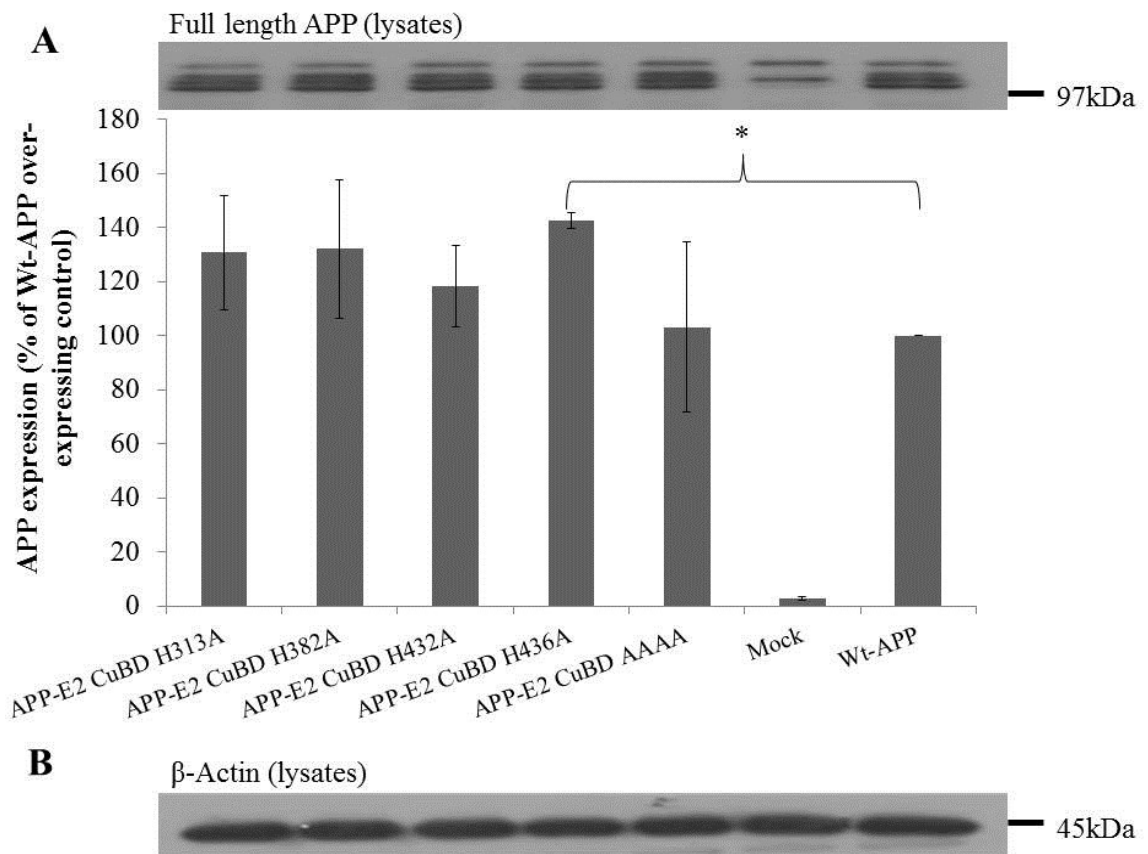


**Figure 3.2. APP expression levels in transiently transfected HEK cell lysates.** The indicated constructs were transiently transfected into HEK cells and lysates were prepared and immunoblotted as described in the Materials and Methods section. **A.** Full-length APP was detected using the anti-APP C-terminal antibody. Results from triplicate immunoblots were quantified and the results are expressed as a percentage of the Wt-APP over-expressing cells (means  $\pm$  S.D.). **B.** Cell lysates were immunoblotted using the anti- $\beta$ -actin antibody in order to confirm equal protein loading. (n=3) \*, significant at  $P \leq 0.05$ .

In order to examine any effects of the E2 CuBD mutations on the proteolysis of APP, the conditioned medium samples were then immunoblotted with the anti-APP 6E10 antibody in order to detect soluble APP $\alpha$  fragments (sAPP $\alpha$ ). The results (Fig. 3.3.) show that, whilst the generation of sAPP $\alpha$  was clearly enhanced in the Wt-APP overexpressing HEK cells and E2 CuBD mutants (relative to the mock control), there was significantly less sAPP $\alpha$  generated by the E2 CuBD mutant constructs compared to the Wt-APP over-expressing cells. The conditioned medium samples were also

immunoblotted with the anti-sAPP $\beta$  1A9 antibody in order to detect sAPP $\beta$ . However, at the levels of APP overexpression achieved by transient transfection, no sAPP $\beta$  could be detected (results not shown).

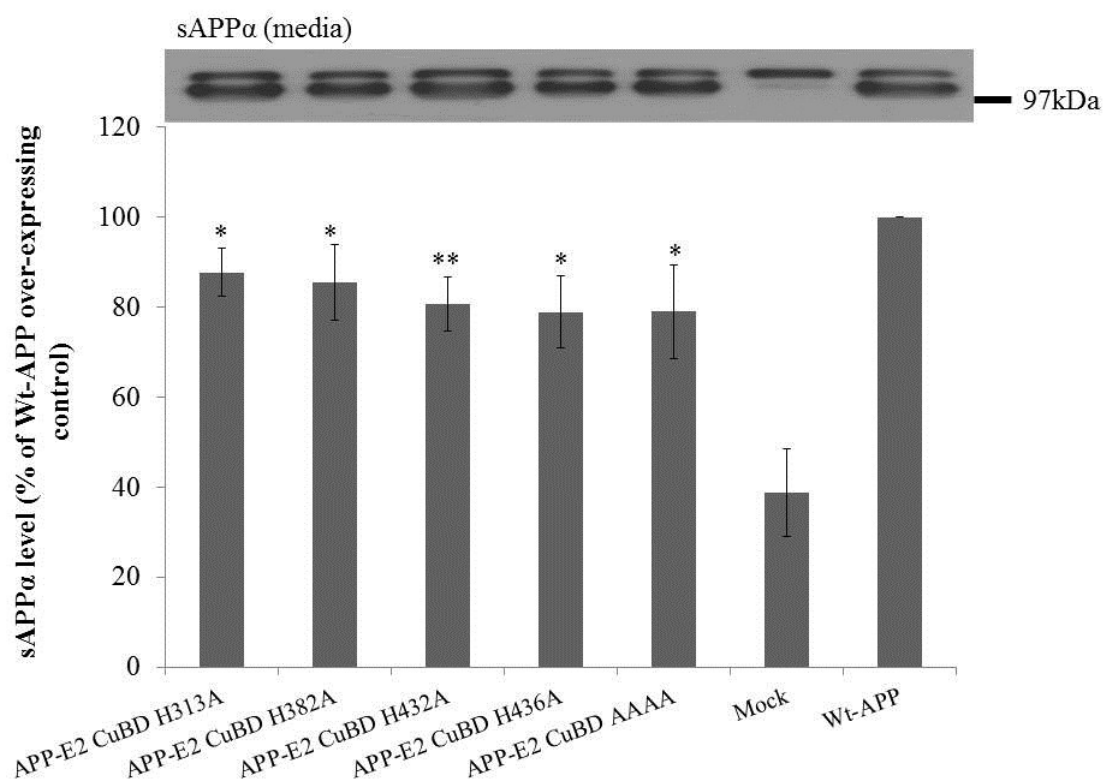


**Figure 3.3. sAPP $\alpha$  levels in medium from transiently transfected HEK cells.** The indicated constructs were transiently transfected into HEK cells and conditioned medium samples were prepared and immunoblotted for sAPP $\alpha$  using antibody 6E10 as described in the Materials and Methods section. Results from triplicate immunoblots were quantified and the results are expressed as a percentage of the sAPP $\alpha$  generated by the Wt-APP over-expressing cells (means  $\pm$  S.D.). \*, significant at  $P \leq 0.05$ ; \*\*, significant at  $P \leq 0.005$

Thus, it is apparent from these results that the transient transfection of the constructs into HEK cells resulted in APP over-expression as would be expected and that, excluding H436A, the histidine to alanine mutations in the APP E2 CuBD made no difference to the levels of APP expression. However, these results indicate that

mutations in the APP E2 CuBD may slightly reduce the non-amyloidogenic processing of APP.

### **3.2. Stable expression and proteolysis of constructs in HEK cells**

For future toxicity experiments it was infeasible to use transiently transfected cells. Therefore, having confirmed that the constructs expressed correctly by transient transfection, stable HEK cell transfectants were also generated. Successfully transfected cells were selected using hygromycin B as described in the Materials and Methods section. In order to monitor APP expression and proteolysis, confluent cells were then incubated for 24h in UltraMEM® and lysate and conditioned medium samples were subsequently prepared (see Materials and Methods).

The lysates were initially immunoblotted using the anti-APP C-terminal antibody in order to detect the APP holoprotein. The results (Fig 3.4A) show that levels of APP were dramatically higher in lysates prepared from cells transfected with Wt-APP and the APP E2 CuBD mutants compared to the mock-transfected cells. Furthermore, there were no significant differences in APP holoprotein expression levels between cells over-expressing Wt-APP and any of the E2 CuBD mutants. Following probing for APP, the blots were stripped and subsequently re-probed for actin which showed equal loading of proteins across the samples (Fig 3.4B).

Previous studies have demonstrated that low concentrations of copper increase sAPP $\alpha$  secretion [98]. In order to determine if the binding of copper to the E2 CuBD of APP might be responsible for these previous observations, conditioned medium samples from the HEK stable transfectants in the current study were also immunoblotted with antibody 6E10 to detect sAPP $\alpha$ .

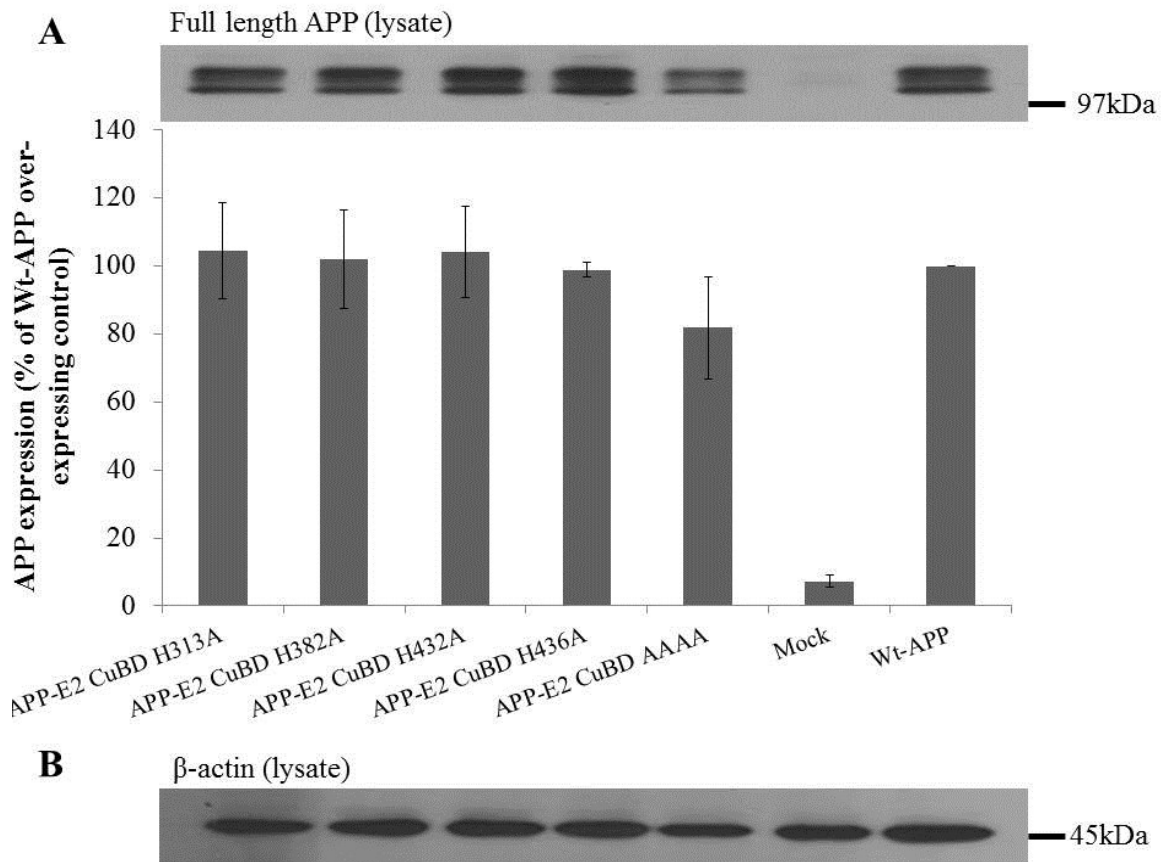


**Figure 3.4. APP expression levels in stably transfected HEK cell lysates.** The indicated constructs were stably transfected into HEK cells and lysates were prepared and immunoblotted as described in the Materials and Methods section. **A.** Full-length APP was detected using the anti-APP C-terminal antibody. Results from triplicate immunoblots were quantified and the results are expressed as a percentage of the Wt-APP over-expressing cells (means  $\pm$  S.D.). **B.** Cell lysates were immunoblotted using the anti- $\beta$ -actin antibody in order to confirm equal protein loading. (n=3)

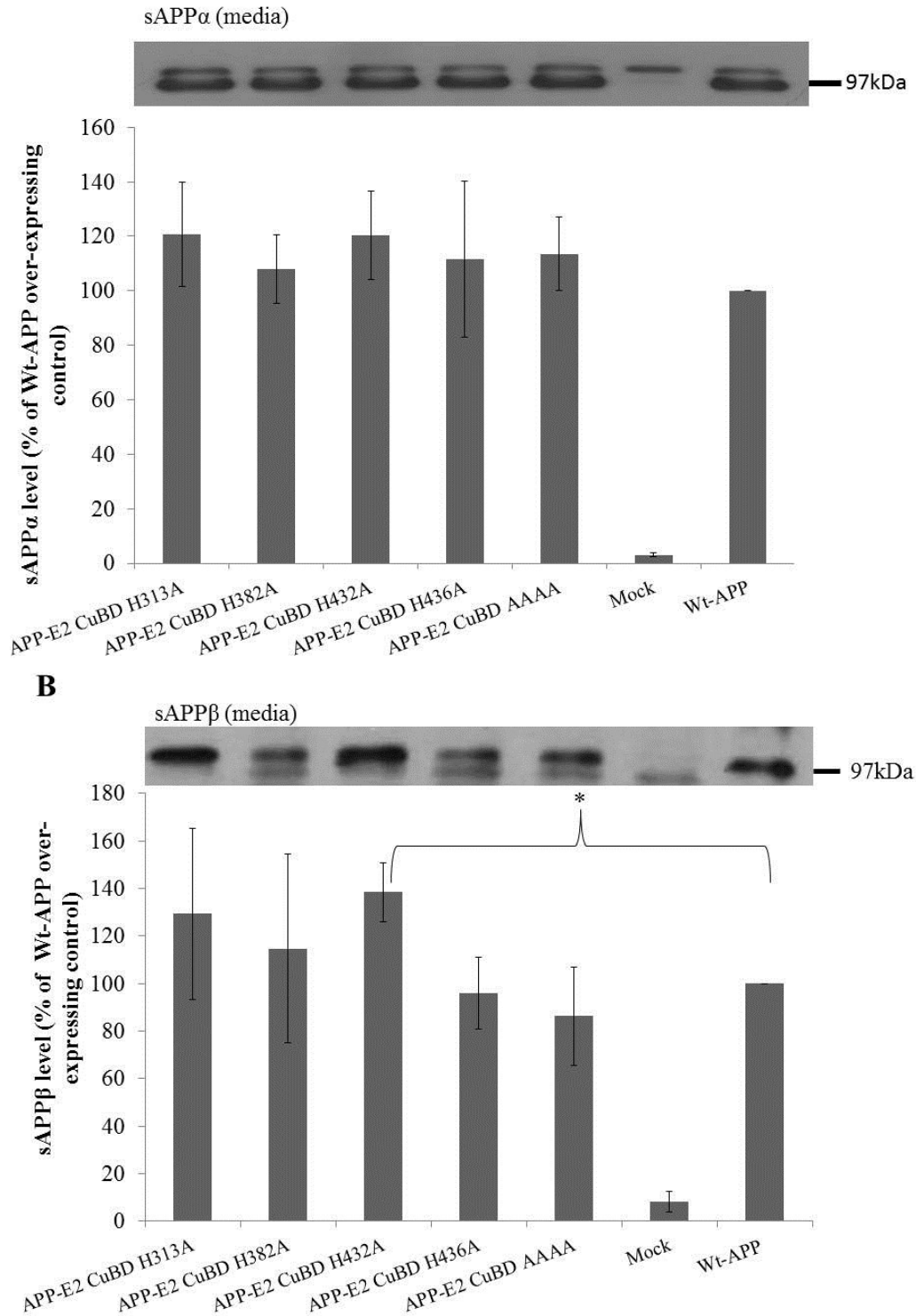


**Figure 3.5. sAPP $\alpha$  and sAPP $\beta$  levels in medium from stably transfected HEK cells.** The indicated constructs were stably transfected into HEK cells and conditioned medium samples were prepared and immunoblotted for **(A)** sAPP $\alpha$  using antibody 6E10 and **(B)** sAPP $\beta$  using anti-sAPP $\beta$  antibody 1A9 (see Materials and Methods). Results from triplicate immunoblots were quantified and the results are expressed as a percentage of the sAPP $\alpha$  or sAPP $\beta$  generated by the Wt-APP over-expressing cells (means  $\pm$  S.D.). (n=3)\*, significant at  $P \leq 0.05$ .

The results (Fig. 3.5A) clearly showed that, whilst the amount of sAPP $\alpha$  generated was much higher in APP-transfected cells than in the mock controls, there were no significant differences between the amount of the fragment produced by Wt-APP over-expressing cells and those transfected with any of the E2 CuBD mutant constructs. Therefore, copper binding to the E2 domain did not impact on the non-amyloidogenic processing of APP in this instance.

The same conditioned medium samples were probed separately for the amyloidogenic pathway proteolytic fragment sAPP $\beta$ , using antibody 1A9 which recognises a neoepitope on sAPP $\beta$  generated by  $\beta$ -secretase cleavage. The results (Fig. 3.5B) again showed that the levels of this fragment were higher in all of the APP over-expressing cell lines compared to the mock control. Only the APP-E2 CuBD H432A construct exhibited elevated sAPP $\beta$  generation relative to the Wt-APP-transfected control (1.38-fold increase).

### **3.3. Stable expression and proteolysis of constructs in SH-SY5Y cells**

The neuroblastoma cell line SH-SY5Y is an extensively used model of AD as it exhibits neuronal-like properties [121]. Therefore, in order to determine the effects of the E2 CuBD mutants in a cell model of relevance to AD and to eliminate any cell-type specific differences, the APP-E2 CuBD mutant constructs were also stably expressed in SH-SY5Y cells. Once stable transfectants had been selected using hygromycin, confluent cells were incubated for 24 h in UltraMEM $\text{\textcircled{R}}$ , and lysates and conditioned medium samples were prepared (see Materials and Methods).

The lysate samples were initially immunoblotted with the anti-APP C-terminal antibody in order to quantify the expression of the various constructs. As observed

previously in HEK cells, the Wt-APP and E2 CuBD domain over-expressing SH-SY5Y cells exhibited dramatically higher APP expression compared to the mock cells (Fig. 3.6A). Of all the E2 CuBD mutants, only APP-E2 CuBD H436A and APP-E2 CuBD AAAA were expressed at levels different to that of the over-expressed wild-type protein (38% and 42% lower, respectively). Immunoblot analysis of actin levels in the cell lysates confirmed equal protein loading (Fig. 3.6B).

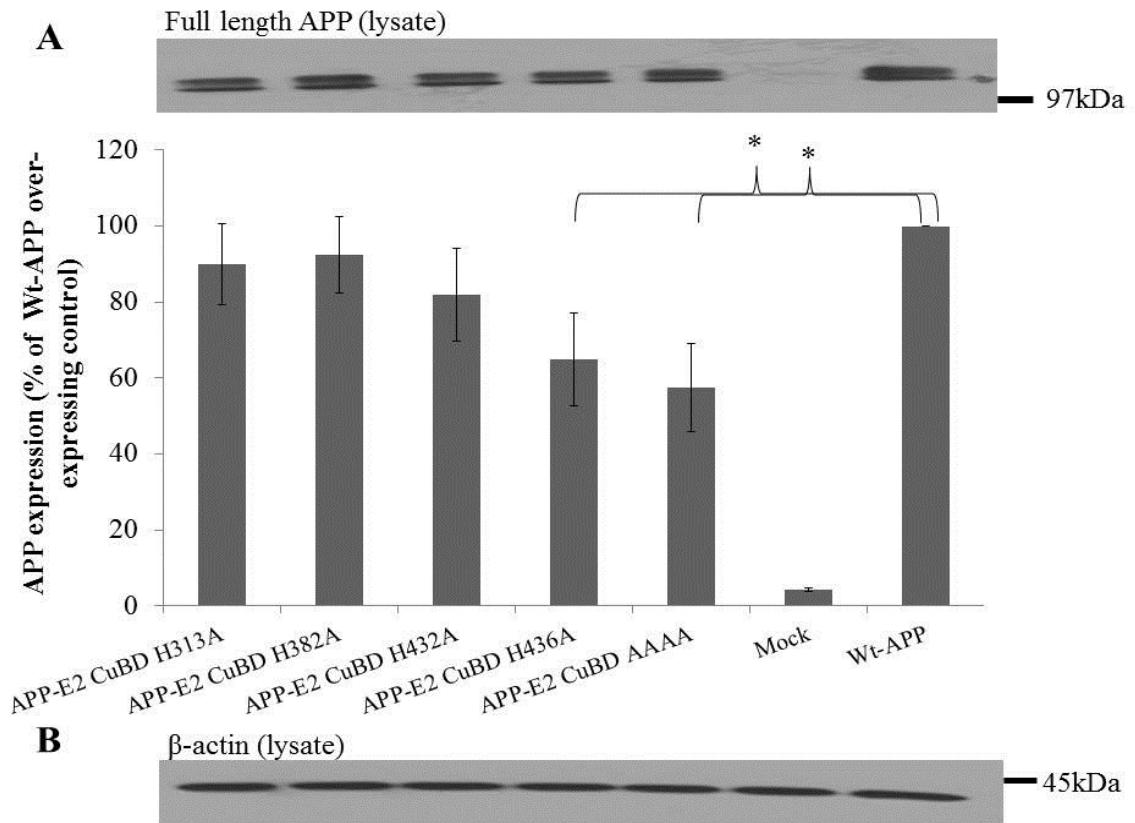


**Figure 3.6. APP expression levels in stably transfected SH-SY5Y cell lysates.** The indicated constructs were stably transfected into SH-SY5Y cells and lysates were prepared and immunoblotted as described in the Materials and Methods section. **A.** Full-length APP was detected using the anti-APP C-terminal antibody. Results from triplicate immunoblots were quantified and the results are expressed as a percentage of the Wt-APP over-expressing cells (means  $\pm$  S.D.). **B.** Cell lysates were immunoblotted using the anti- $\beta$ -actin antibody in order to confirm equal protein loading. (n=3)\*, significant at  $P \leq 0.05$ .

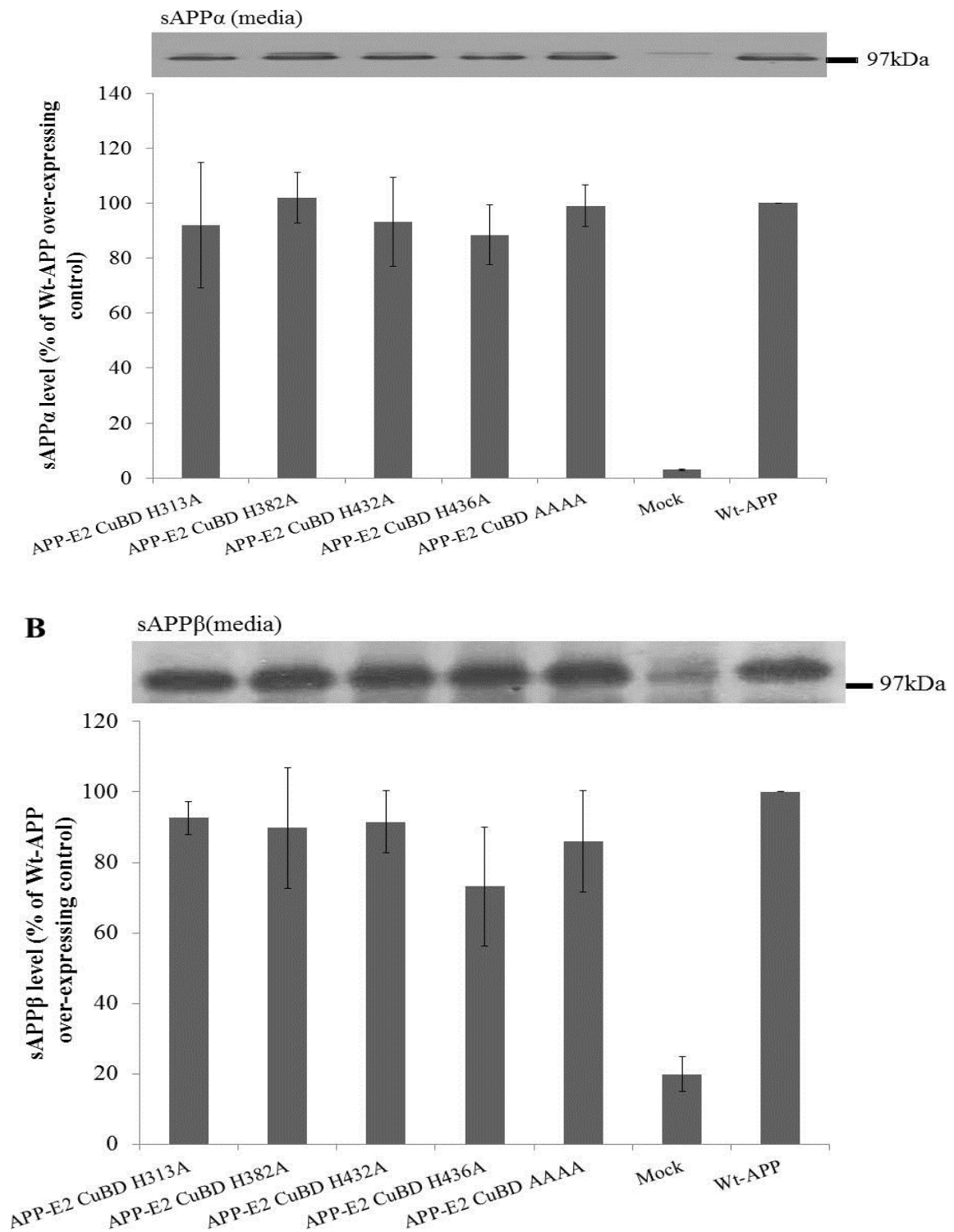


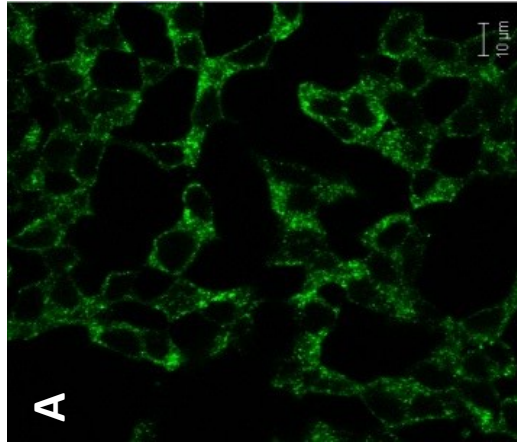
**Figure 3.7. sAPP $\alpha$  and sAPP $\beta$  levels in medium from stably transfected SH-SY5Y cells.** The indicated constructs were stably transfected into SH-SY5Y cells and conditioned medium samples were prepared and immunoblotted for (A) sAPP $\alpha$  using antibody 6E10 and (B) sAPP $\beta$  using anti-sAPP $\beta$  antibody 1A9 (see Materials and Methods). Results from triplicate immunoblots were quantified and the results are expressed as a percentage of the sAPP $\alpha$  or sAPP $\beta$  generated by the Wt-APP over-expressing cells (means  $\pm$  S.D.). (n=3)

The conditioned medium samples from the SH-SY5Y stable transfectants were then immunoblotted with antibody 6E10 in order to quantify sAPP $\alpha$ . The results (Fig. 3.7A) revealed no significant changes in sAPP $\alpha$  generation associated with the introduction of mutations in the E2 CuBD. Immunoblotting of the same samples with antibody 1A9 (Fig. 3.7B) also showed no change in the generation of sAPP $\beta$  in the E2 CuBD mutant expressing cells. Thus, it is apparent that, despite some variation in the expression levels of the APP constructs, there were no significantly different changes observed in either the amyloidogenic or non-amyloidogenic processing of the proteins.

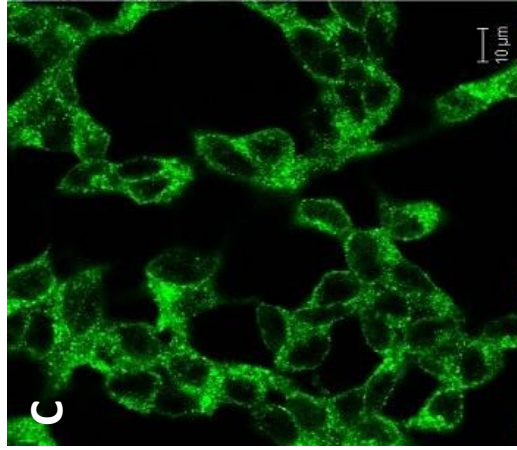
### **3.4. Subcellular localisation of constructs in stable SH-SY5Y transfectants**

In order to determine whether altered copper binding to the APP E2 CuBD affected the subcellular localisation of APP, SH-SY5Y cells stably transfected with either Wt-APP or the APP-E2 CuBD constructs were subjected to immunofluorescence as described in Materials and Methods. The antibody employed, ab15272 (Abcam, Cambridge, UK), recognises an epitope within amino acids 44-62 of APP and, therefore, detects the N-terminal region of all three major APP isoforms. Nuclei were co-stained with DAPI.

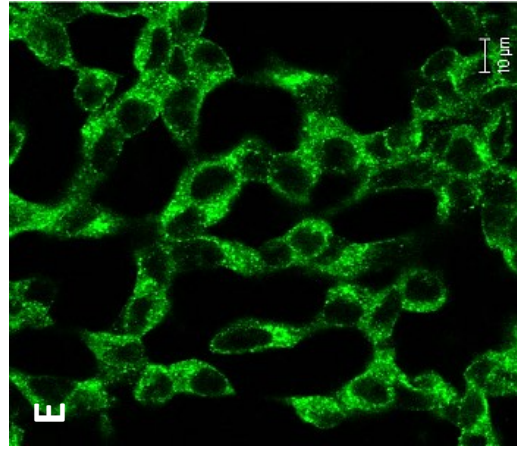
pIREShyg Mock



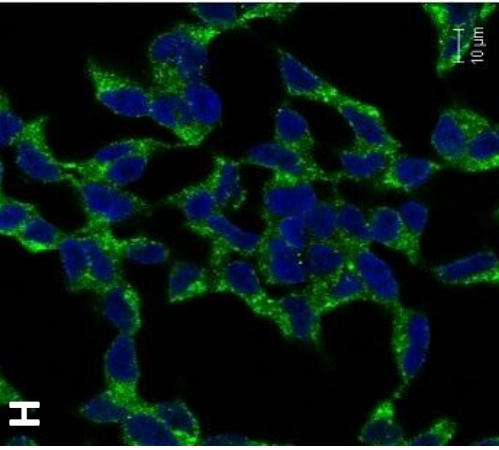
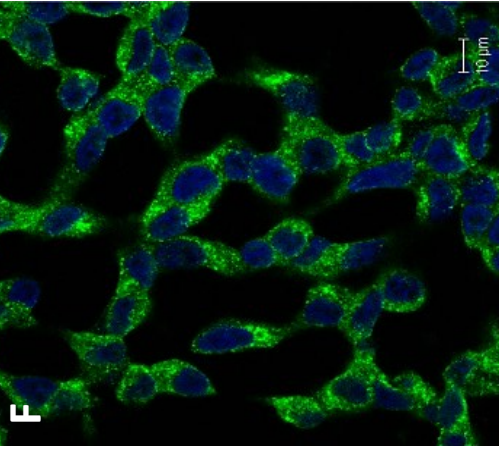
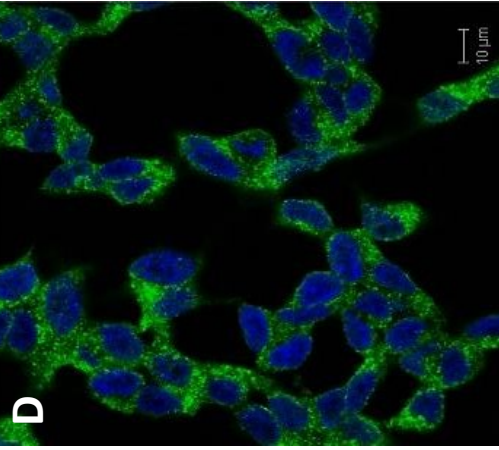
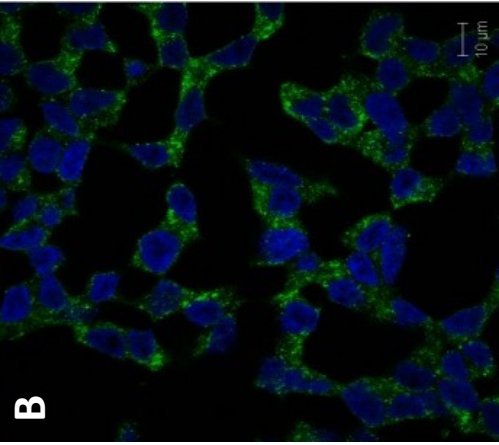
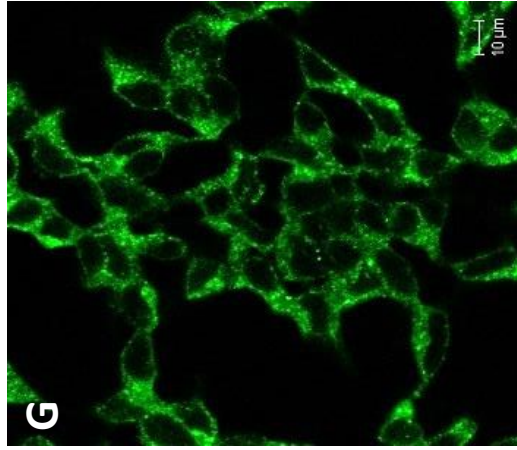
Wt-APP



E2 CuBD H313A



E2 CuBD H382A



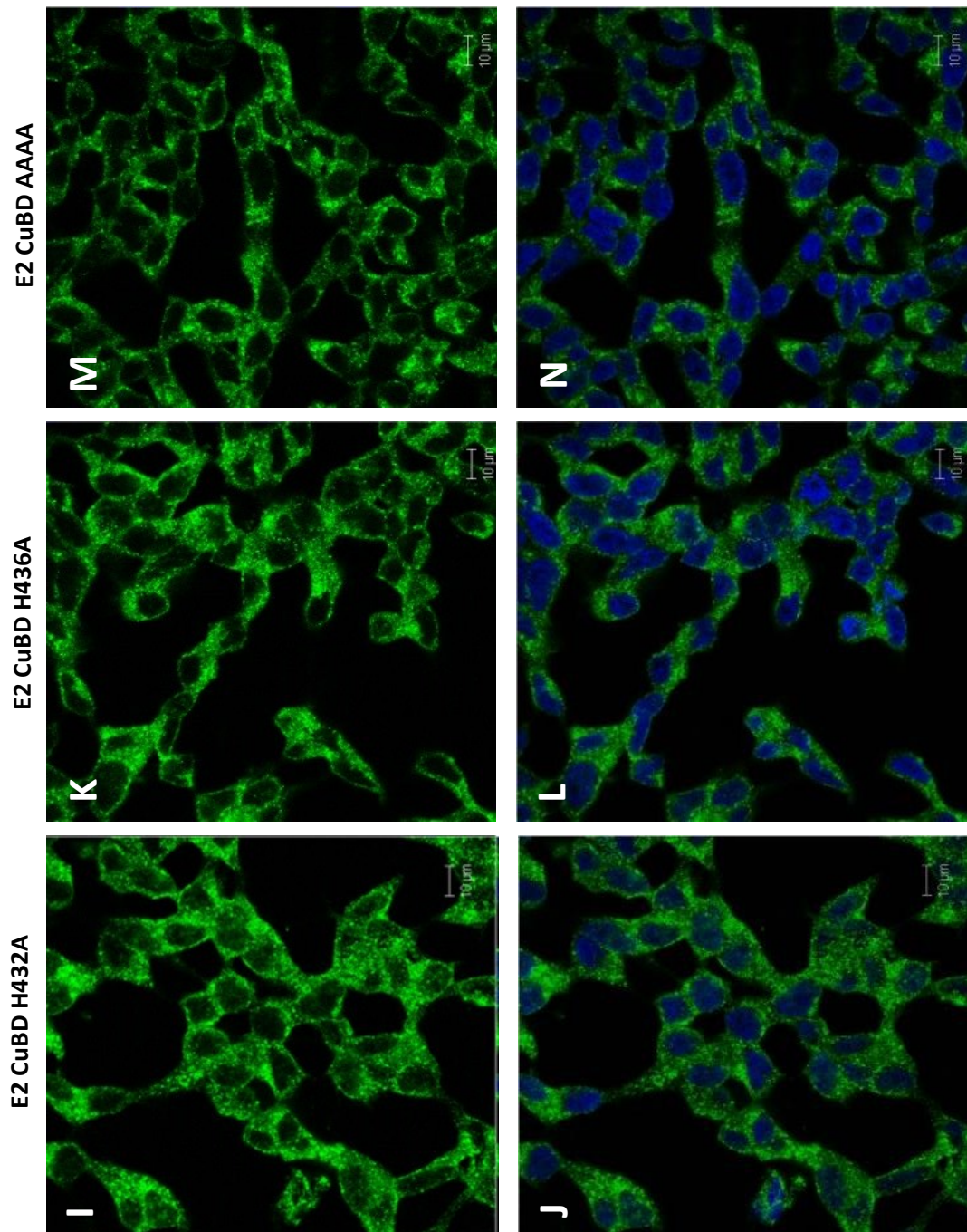


**Figure 3.8. Immunofluorescence detection of APP expression in SH-SY5Y stable transfectants.** Cells were cultured on coverslips and fixed and stained with ab15272 as described in the Materials and Methods section. **A, C, E, G, I, K, M,** detection of APP. **B, D, F, H, J, N,** co-detection of DAPI stained nuclei and APP. (n=1)

The results (Fig. 3.8) show enhanced fluorescence in the APP over-expressing cell lines compared to the mock-transfected cells. Clearly endogenous APP was also detected in the mock cells. In all of the cell lines, APP expression was detected mainly as peri-nuclear fluorescence consistent with a predominantly ER/Golgi localisation. The pattern of fluorescence did not differ substantially between the Wt-APP over-expressing cells and any of the APP E2 CuBD mutant cells indicating that copper binding to the E2 domain did not alter the subcellular localisation of APP.

### **3.5. Role of the APP E2 CuBD in cytotoxicity**

Previous studies have indicated that the APP E1 CuBD might be involved in the regulation of copper-induced neurotoxicity [102]. In the current study, it was hypothesized that the E2 CuBD domain may act in a similar manner.

#### **3.5.1. Free copper-mediated neurotoxicity**

Although the concentration of copper in the circulation is much lower, copper concentrations of up to 400  $\mu\text{M}$  have been observed in amyloid plaques [104]. Furthermore, previous studies have employed free copper concentrations of up to 250  $\mu\text{M}$  when studying the effect of metal toxicity on neuronal cell lines [35]. As a result, in this section of the current study, copper concentrations of up to 200  $\mu\text{M}$  were considered appropriate. HEK and SH-SY5Y cells stably transfected with either Wt-APP or the various APP E2 CuBD mutants were grown to confluence and then incubated for 48 h in the absence or presence of  $\text{CuSO}_4 \cdot 5\text{H}_2\text{O}$  (0-200  $\mu\text{M}$ ). Cell viability was then determined using the CellTiter 96® AQueous One Cell proliferation Assay as described in the Materials and Methods section. In the case of HEK cells, the results (Fig. 3.9) show that, following treatment with the lower 50  $\mu\text{M}$

copper concentration, the viability of the mock transfectants actually increased significantly. Although only small, this increase in viability may have been due to a minor growth stimulating effect of copper at lower concentrations compared to 200  $\mu\text{M}$  metal at which concentration the viability of the mock transfectants was reduced (82% of the untreated mock-transfectants). In terms of the APP transfecting cells, metal-mediated toxicity was only observed at the highest copper concentration (200  $\mu\text{M}$ ). At this concentration, viability in Wt-APP transfecting cells was significantly lower than mock transfectants (81% of mock transfectants in 200 $\mu\text{M}$  copper) which suggests that APP potentiates copper induced neurotoxicity. Of the APP-E2 CuBD mutants, H382A significantly reversed the reduction of cell viability observed in Wt-APP transfectants returning viability to the levels observed in mock transfectants. This indicates that, as hypothesised, the APP E2 CuBD may regulate copper induced toxicity.

In terms of the SH-SY5Y stable transfectants, the results (Fig. 3.10) revealed that none of the copper concentrations employed actually resulted in significant cytotoxicity. It could, therefore, not be determined whether or not APP had any effect on toxicity in this context.

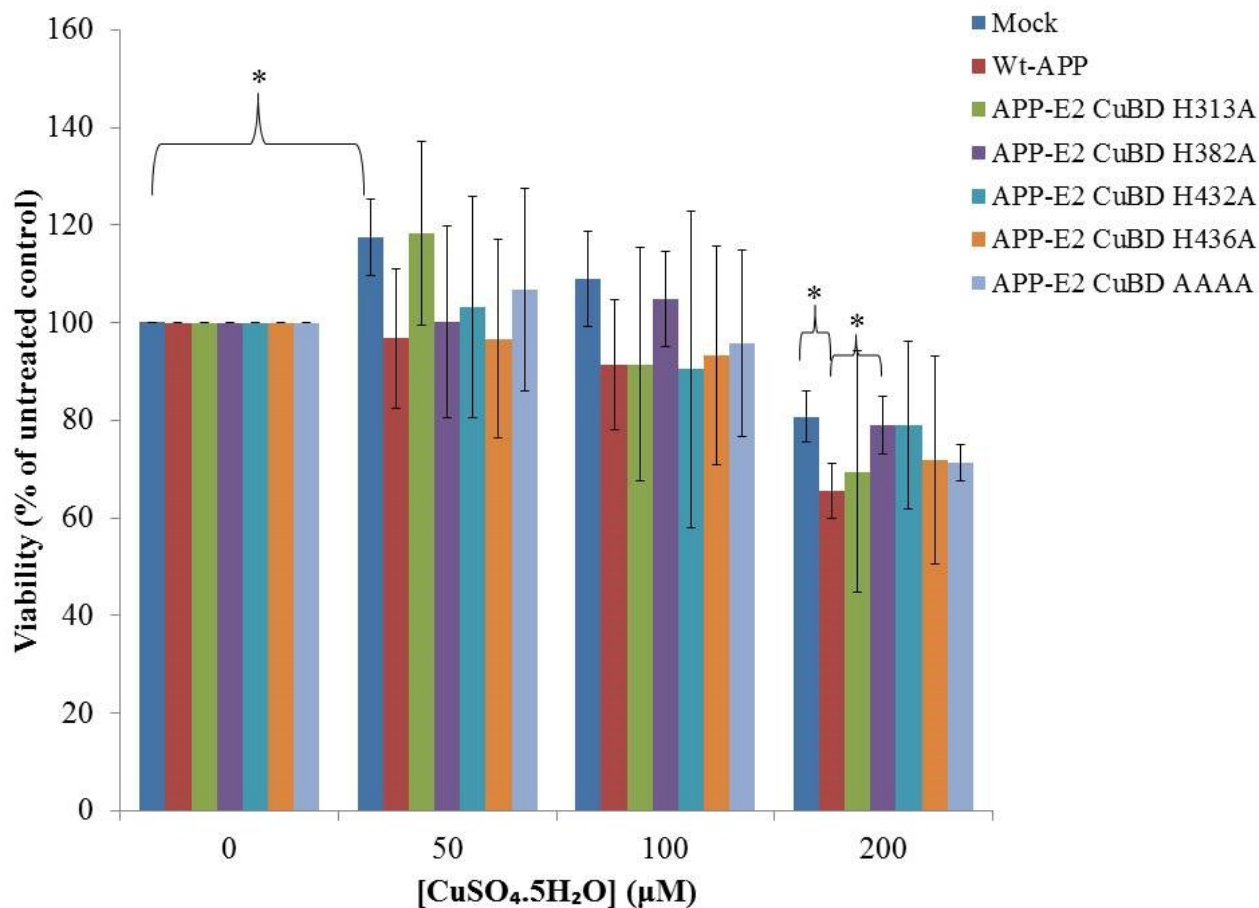


**Figure 3.9. The effect of free copper on the viability of HEK cell stable transfectants.** The cells were grown to confluence and then treated for 48 h with the indicated concentrations of CuSO<sub>4</sub>.5H<sub>2</sub>O. The cell viability was then determined using the CellTiter 96® AQueous One Cell proliferation Assay as described in the Materials and Methods section. The results for each cell line are expressed relative to the viability in the absence of copper of that particular cell line. The results shown are means ± S.D. (n=3). \*, significant at P≤0.05.

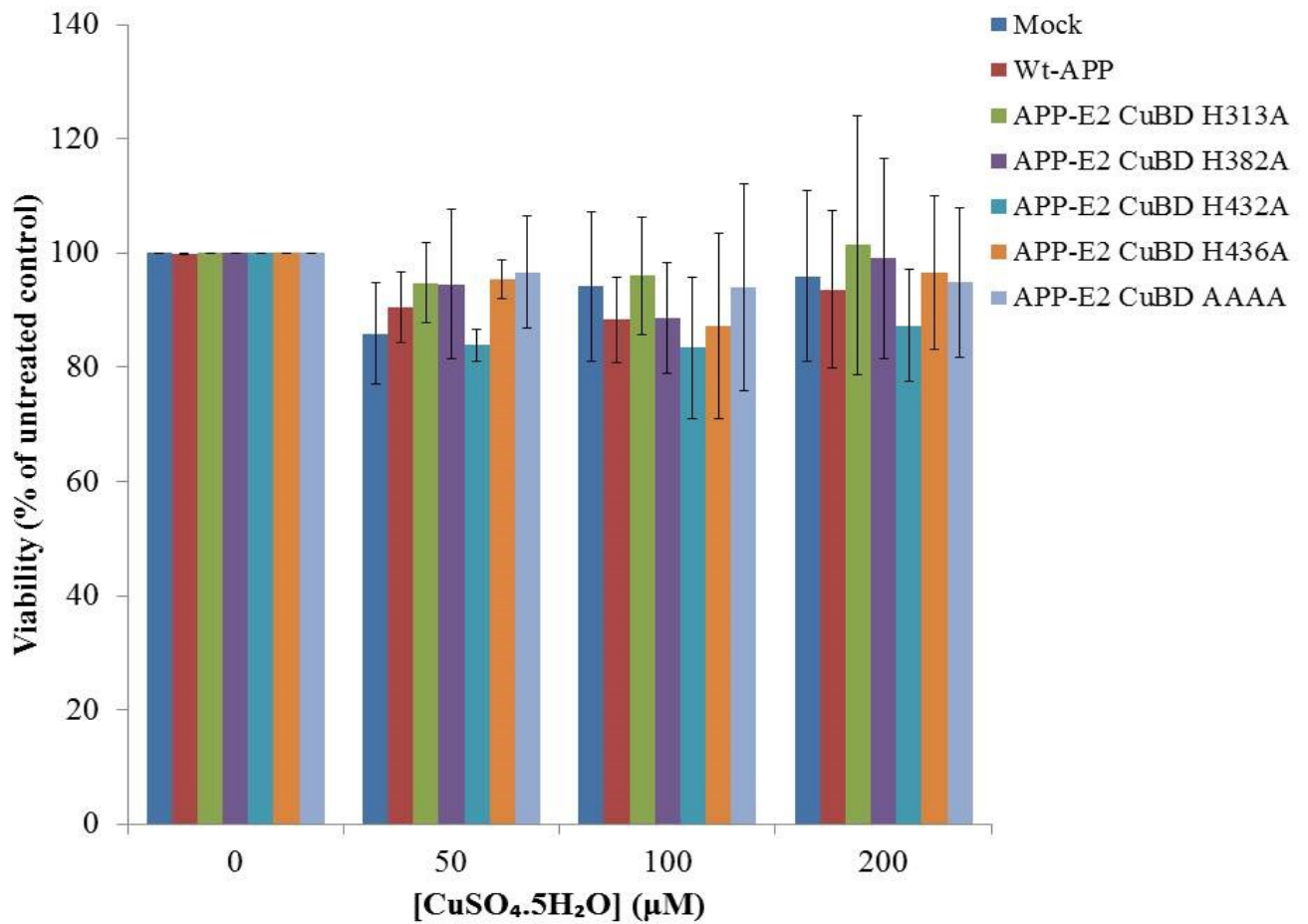


**Figure 3.10. The effect of free copper on the viability of SH-SY5Y cell stable transfectants.** The cells were grown to confluence and then treated for 48 h with the indicated concentrations of CuSO<sub>4</sub>.5H<sub>2</sub>O. The cell viability was then determined using the CellTiter 96® AQueous One Cell proliferation Assay as described in the Materials and Methods section. The results for each cell line are expressed relative to the viability in the absence of copper of that particular cell line. The results shown are means ± S.D. (n=3).

### **3.5.2. Copper-glycine-mediated neurotoxicity**

In the preceding section, free copper was employed in order to examine the effect of APP on metal-mediated cytotoxicity. However, the majority of copper in the brain and elsewhere in the body exists in a protein bound form [85]. In order to improve the physiological relevance of the current study, the effect of glycine-complexed copper on the viability of the various HEK and SH-SY5Y APP stable transfectants was also examined.

Cells were grown to confluence and then treated with the indicated concentrations of glycine-copper complexes for 24 h (the concentration refers to the final metal concentration in the culture medium). Cell viability was once more determined using the CellTiter 96® AQueous One Cell proliferation Assay as described in the Materials and Methods section.

Before examining the effect of any of the APP stable transfections on toxicity, metal dose-response curves were established in mock-transfected cells. In relation to the HEK cells, the dose response results (Fig. 3.11) show that cells were resistant to the lowest metal concentration of 150  $\mu\text{M}$  but that toxicity increased in a dose-dependent manner right up to 700  $\mu\text{M}$  copper. Having established that the minimum copper concentration required to kill HEK cells was 250  $\mu\text{M}$ , this 'threshold' toxicity concentration, along with one higher metal concentration (600  $\mu\text{M}$ ) were used to treat the various APP stably-transfected HEK cell lines. As described above, confluent cells were incubated for 24 h in the presence of the indicated copper-glycine complex concentrations and cell viability was subsequently determined as described in the Materials and Methods section.

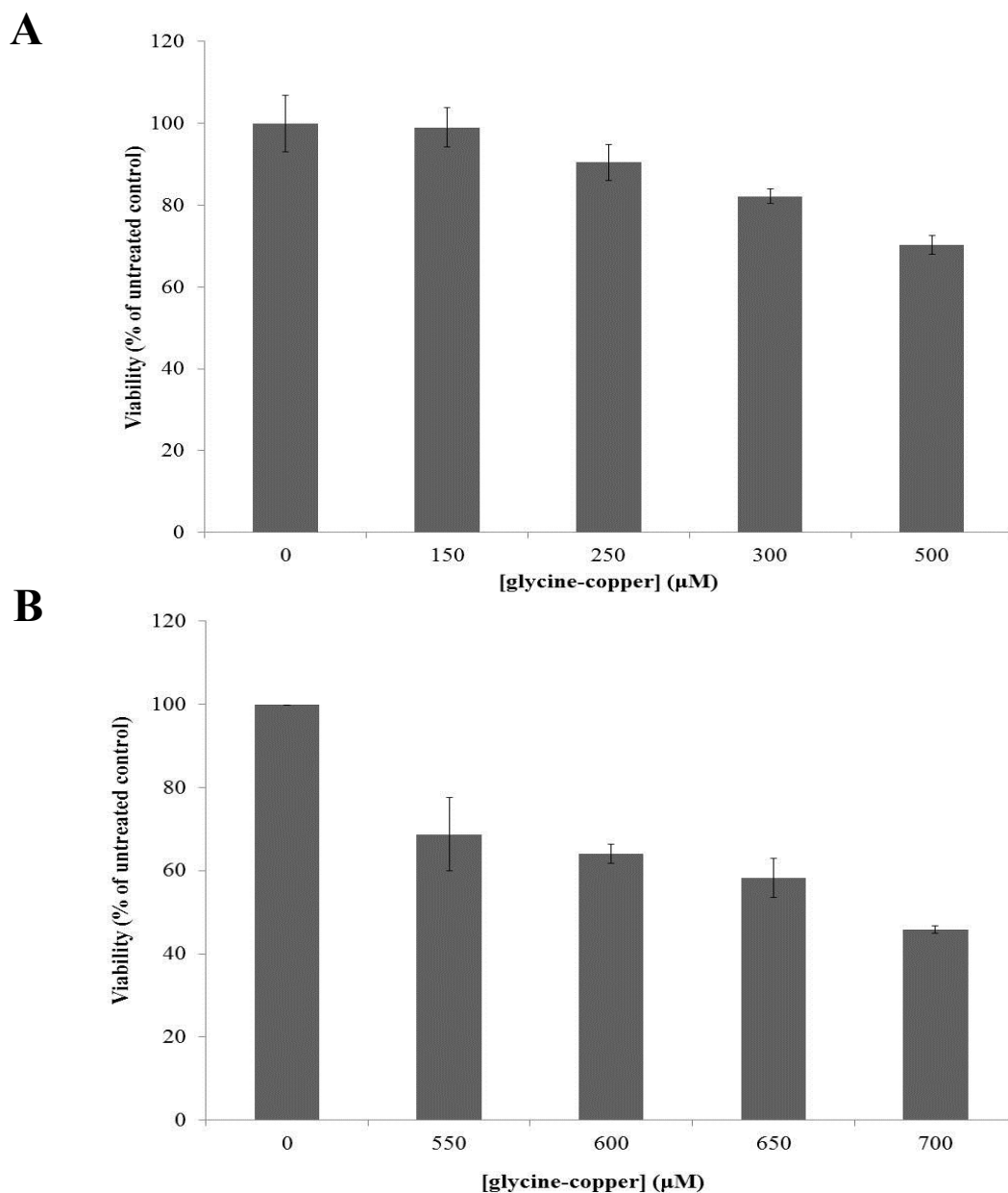


**Figure 3.11. The effect of glycine-complexed copper on the viability of mock-transfected HEK cells.** The cells were grown to confluence and then treated for 24 h with the indicated concentrations of metal in the form of glycine-complexed copper chloride. The cell viability was then determined using the CellTiter 96® AQueous One Cell proliferation Assay as described in the Materials and Methods section. Panels **A** and **B** represent data from separate experiments using different metal concentrations. The results shown are means  $\pm$  S.D. (n=3).

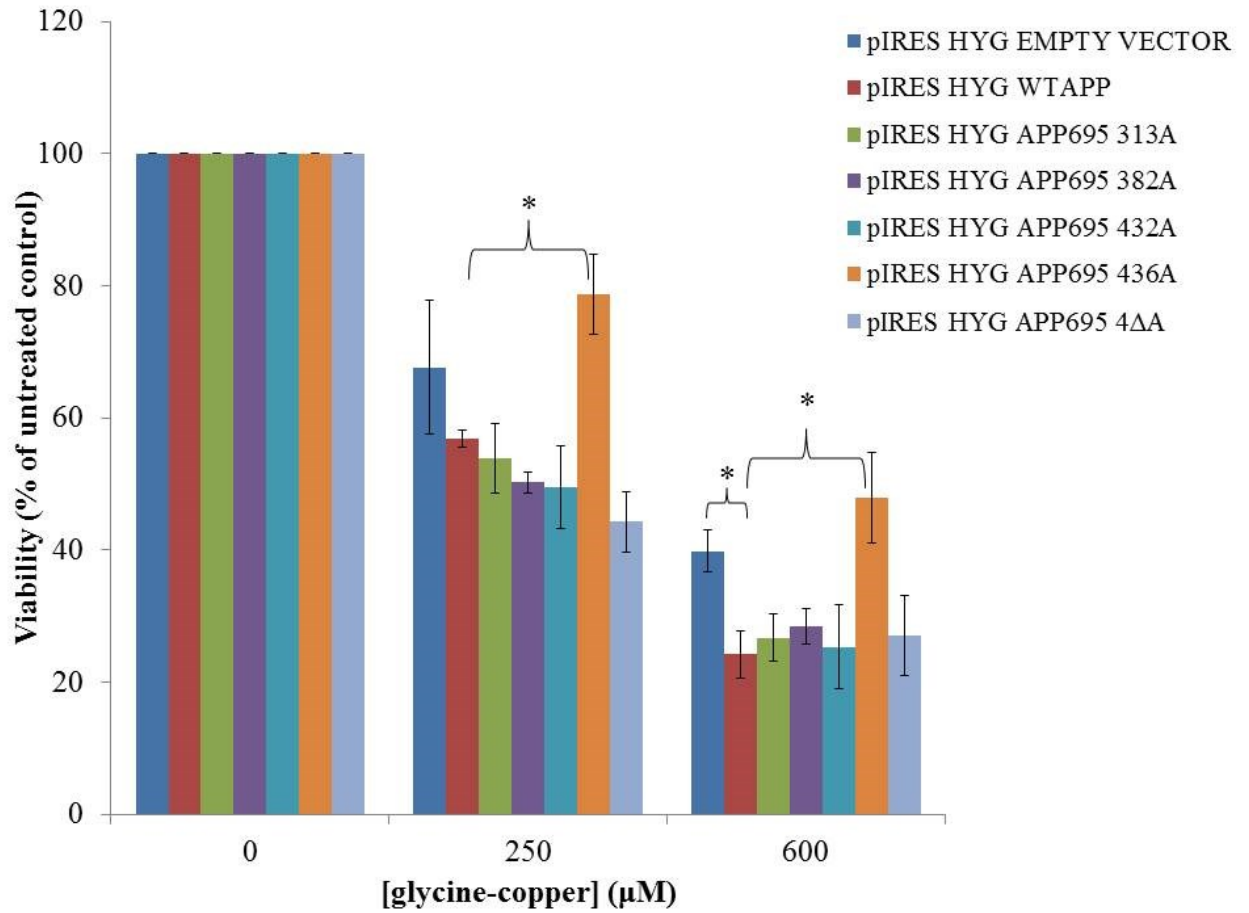


**Figure 3.12. The effect of glycine-complexed copper on the viability of HEK cell stable transfectants.** The cells were grown to confluence and then treated for 24 h with the indicated concentrations of metal in the form of glycine-complexed copper chloride. The cell viability was then determined using the CellTiter 96® AQueous One Cell proliferation Assay as described in the Materials and Methods section. The results for each cell line are expressed relative to the viability in the absence of copper of that particular cell line. The results shown are means  $\pm$  S.D (n=3). \*, significant at  $P \leq 0.05$ .

The results (Fig. 3.12) demonstrated a clear reduction in the viability of mock-transfected HEK cells at both 250  $\mu\text{M}$  and 600  $\mu\text{M}$  copper concentrations (68% and 40% respectively). Cells over-expressing Wt-APP exhibited a significant decrease in viability at 600  $\mu\text{M}$  copper compared to the mock-transfected HEK cells. Most of the APP-E2 CuBD mutant-transfected cells exhibited viability unchanged from that of the Wt-APP transfected cells at both of the metal concentrations employed, indicating that the E2 CuBD domain was not responsible for the increased sensitivity of APP-transfected cells to copper toxicity. The one exception in this respect was that of the APP-E2 CuBD H436A mutant which exhibited viability indistinguishable from that of the mock-transfected cells at both 250  $\mu\text{M}$  and 600  $\mu\text{M}$  copper concentrations. Thus, it would appear that histidine 436 may well be involved in mediating the toxic effects of glycine-copper complexes although it is not clear why the quadruple substitution mutant, APP-E2 CuBD AAAA did not exhibit a similar effect.

Having determined the effects of the various APP stable transfections on glycine-copper mediated toxicity to HEK cells, similar results were conducted in SH-SY5Y cells. Initially, copper toxicity does response was examined in mock-transfected cells. The results (Fig. 3.13) show that SH-SY5Y cells were considerably more resilient than HEK cells to glycine-copper-induced toxicity with only metal concentrations greater than 500  $\mu\text{M}$  generating appreciable cell death.

On the basis that APP might actually enhance toxicity (as seen for HEK cells), one sub-toxic metal concentration along with a known toxic concentration (250  $\mu\text{M}$  and 600  $\mu\text{M}$ ) were then utilised in order to examine the effects of APP on metal-induced toxicity in SH-SY5Y cells. As previously, the various mock- and APP-transfected SH-SY5Y cell lines were incubated with the indicated metal concentrations for 24 h before quantifying cell viability (see Materials and Methods).

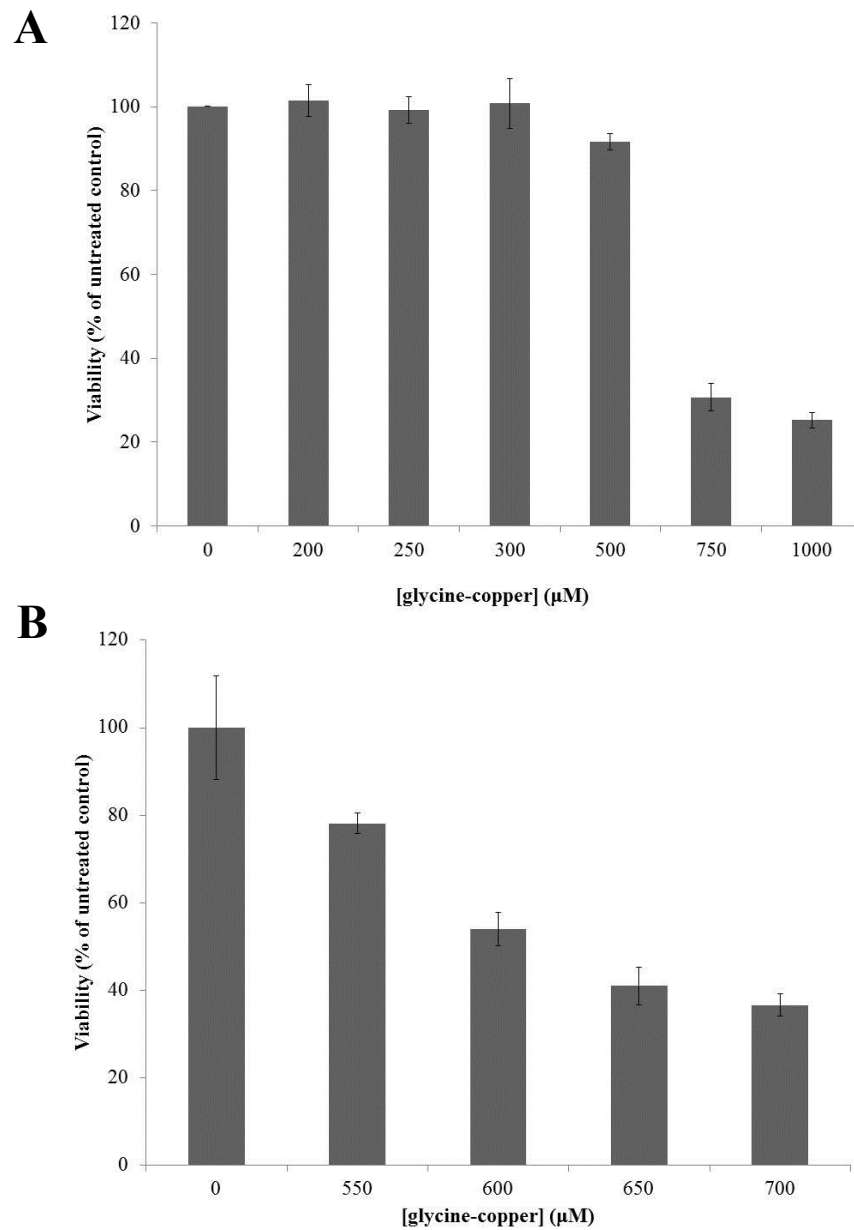


**Figure 3.13. The effect of glycine-complexed copper on the viability of mock-transfected SH-SY5Y cells.** The cells were grown to confluence and then treated for 24 h with the indicated concentrations of metal in the form of glycine-complexed copper chloride. The cell viability was then determined using the CellTiter 96® AQueous One Cell proliferation Assay as described in the Materials and Methods section. Panels **A** and **B** represent data from separate experiments using different metal concentrations. The results shown are means  $\pm$  S.D (n=3).

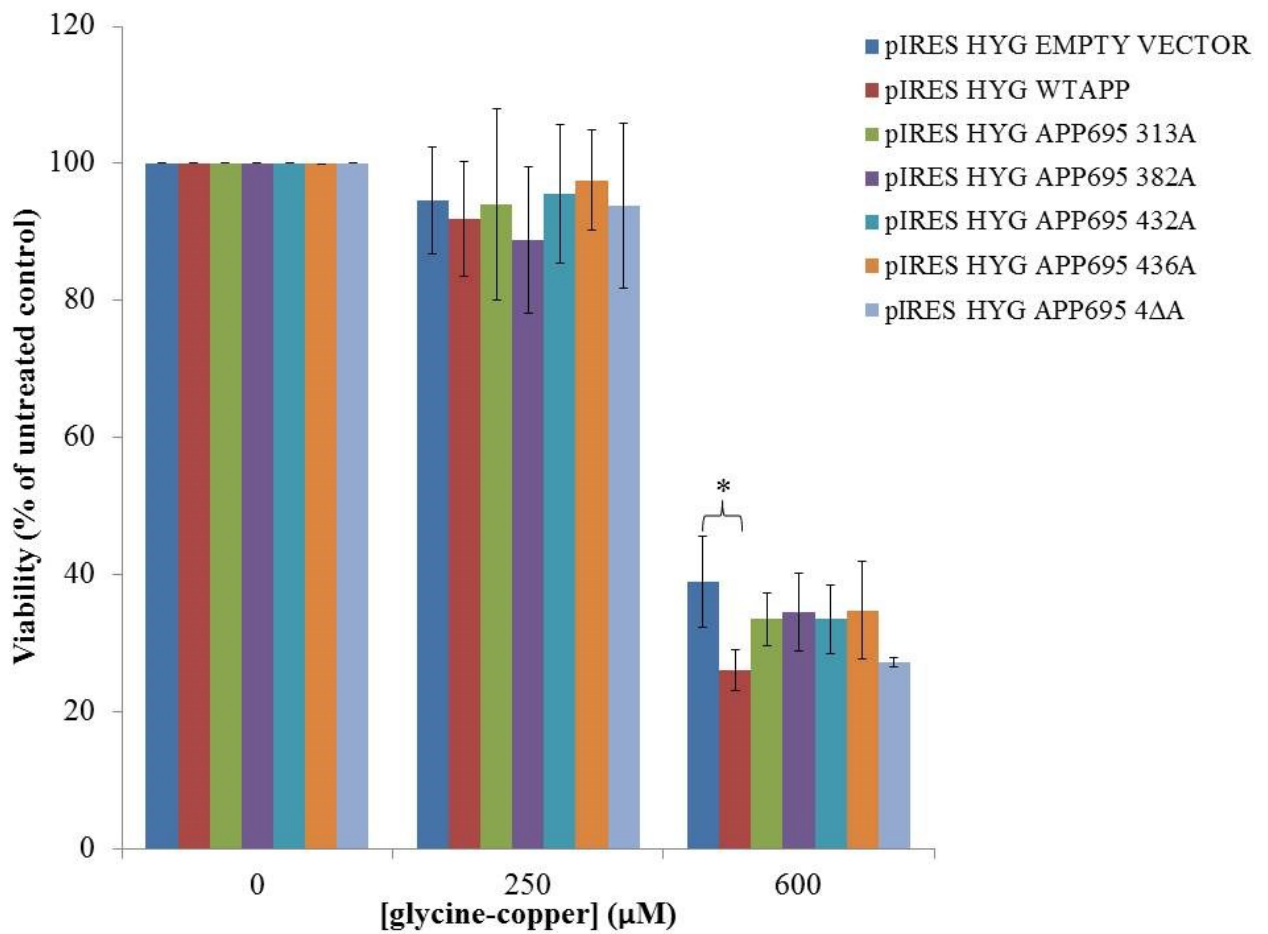


**Figure 3.14. The effect of glycine-complexed copper on the viability of SH-SY5Y cell stable transfectants.** The cells were grown to confluence and then treated for 24 h with the indicated concentrations of metal in the form of glycine-complexed copper chloride. The cell viability was then determined using the CellTiter 96® AQueous One Cell proliferation Assay as described in the Materials and Methods section. The results for each cell line are expressed relative to the viability in the absence of copper of that particular cell line. The results shown are means  $\pm$  S.D. (n=3). \*, significant at  $P \leq 0.05$ .

The results (Fig. 3.14) demonstrated, as might have been expected from the previous dose-response experiment, a lack of glycine-copper-induced cytotoxicity at the lower, 250  $\mu$ M, metal concentration. In contrast, at the higher, 600  $\mu$ M, concentration, all of the cell lines exhibited major decreases in viability. As observed previously, the viability of the mock-transfected cells at this higher metal concentration was greater than that of the Wt-APP-transfected cells suggesting that the protein increases the sensitivity of the cells to metal toxicity. Mutating the APP-E2 CuBD did not prevent the increase in toxicity observed in the Wt-APP-transfected cells. This further demonstrates that this domain is not essential for the toxic effect of Wt-APP in increased copper concentrations.

### **3.6. Summary**

Initially, all of the APP constructs were transiently expressed in HEK cells where the holoprotein expression was equal between constructs with the exception of the APP-E2 CuBD H436A protein which was expressed significantly more highly relative to the over-expressed wild-type protein. The levels of sAPP $\alpha$  generated from all of the APP-E2 CuBD mutant proteins were significantly lower than that produced from the over-expressed wild-type protein. No sAPP $\beta$  could be detected in conditioned medium from the transient transfectants.

In terms of the stable transfectants, the expression of the APP holoprotein was identical in all of the HEK cell lines as were the levels of sAPP $\alpha$  generated. The only significant change was a small increase in the amount of sAPP $\beta$  generated from the APP-E2 CuBD H432A protein. In the SH-SY5Y stable transfectants, the expression of APP-E2 CuBD H436A was slightly lower than that of the over-expressed wild-type

protein but the generation of sAPP $\alpha$  and sAPP $\beta$  from the mutant constructs was identical to that from the over-expressed wild-type protein.

Immunofluorescence detection of the constructs in stably transfected SH-SY5Y cells showed a predominant peri-nuclear staining which did not appear different between the over-expressed wild-type protein and any of the mutant constructs.

Finally, the copper toxicity studies using free copper (copper sulphate) revealed that SH-SY5Y cells were more resilient to this metal than the HEK cells, showing no cell death at the concentrations used. The viability of the mock-transfected HEK cells was significantly decreased at 200  $\mu$ M copper; an effect which was enhanced in the presence of over-expressed Wt-APP. The toxic effect of Wt-APP was reversed by the APP-E2 CuBD H382A mutation.

When glycine-complexed copper was used instead of free copper, Wt-APP again increased the sensitivity of HEK cells to metal toxicity. In these latter experiments, the toxic effect of APP was reversed by the APP-E2 CuBD H436A mutation. In contrast, whilst Wt-APP also enhanced glycine-copper toxicity in the SH-SY5Y stable transfectants, this effect was not reversed by any of the E2 CuBD mutations.

## **4. Discussion**

## **4.1. Discussion**

The APP-E2 CuBD is a novel copper binding site, for which the function is currently unknown. The main aim of this project was, therefore, to analyse the role of the APP-E2 CuBD in APP expression, proteolysis, copper induced neurotoxicity and localisation. The APP-E2 CuBD consists of co-ordinating histidine residues at positions 313, 382, 432 and 436 located in three  $\alpha$ -helices and which binds copper with a strong affinity ( $\leq 13\text{nM}$ ). Determining the role of this binding site will help to elucidate the relationship between copper dyshomeostasis and AD, and may provide novel therapeutic targets.

Previous studies have shown that increased copper alters APP expression and proteolysis [98]. The amyloid cascade hypothesis remains a key theory in the pathogenesis of AD with the majority of therapeutic interventions geared towards reducing  $A\beta$  levels in the brain [122]. Therefore, the initial aim of this project was to determine if the APP-E2 CuBD influences the expression and proteolysis of APP. To do this, APP<sub>695</sub> mutants containing single histidine to alanine mutations in the E2 CuBD copper binding residues (313, 382, 43, 436) and a quadruple mutation were overexpressed in HEK and SH-SY5Y cells by two methods, transient and stable overexpression. The mutant constructs were overexpressed alongside ‘mock’ (pIRESHyg empty vector) and Wt-APP<sub>695</sub> transfections as negative and positive controls.

### **4.1.1. APP expression**

Transient and stable overexpression of APP-E2 CuBD mutants resulted in no consistent difference in APP expression levels relative to Wt-APP. Any variances in APP levels observed were cell line specific, indicating that APP expression is not

influenced by the APP-E2 CuBD. Previous studies have shown that copper overload significantly up regulates APP mRNA levels in cells, which suggests that copper acts as a transcriptional regulator of the *APP* gene [95]. A putative copper responsive element in the *APP* promoter region has been identified which reduced APP levels by 80% when deleted [96]. Thus, it is more likely that copper influences APP expression through a copper response element in the promoter region, rather than binding to the E2-CuBD.

The current study quantified APP holoprotein expression in cell lysates, however APP mRNA was not analysed. Bellingham *et al.* [96] showed an 80% decrease in mRNA with a decrease of APP protein in copper deficient cells, which was associated with a 75% reduction in APP promoter activity. However Cater *et al.* [94] found that APP protein expression remained constant despite a decrease in mRNA, indicating that copper deficiency decreases transcription but increases translation. Future work may include quantifying the APP mRNA in cells transfected with APP-E2 CuBD mutants using real-time RT-PCR to determine if this domain mediates copper induced differences in *APP* translation.

#### **4.1.2. APP proteolysis**

Once APP expression levels had been determined, the next aim was to determine if the APP-E2 CuBD modulated APP proteolysis. Previously, copper concentrations between 20 and 50  $\mu\text{M}$  have been shown to increase non-amyloidogenic APP processing by  $\approx 200\%$  relative to basal levels; the increase was only 50% of the basal level when cells were co-incubated with the metal and a copper chelator [98]. In contrast, copper deficiency stimulates amyloidogenic processing and the co-localisation of copper and APP to lipid rafts [100]. It is currently not known

how copper increases non-amyloidogenic processing, however it is hypothesised that metal binding to APP stimulates a conformational change that permits differential access to enzymes [98] or trafficking proteins such as Fe65 or Sor/La [119]. In the current study, immunoblotting of conditioned media from the stable HEK and SH-SY5Y transfectants revealed that Wt-APP overexpression dramatically increased sAPP $\alpha$  and sAPP $\beta$  levels relative to the cognate mock-transfected controls. However, there was no consistent alteration in sAPP $\alpha$  or sAPP $\beta$  shedding in cells stably expressing APP-E2 CuBD mutants compared to Wt-APP expressing cells. This result was important as it demonstrates that the APP-E2 CuBD does not seem to regulate APP proteolysis. Conversely, HEK cells transiently overexpressing the APP-E2 CuBD mutants exhibited significantly decreased sAPP $\alpha$  production relative to Wt-APP-transfected cells, although there was no reciprocal increase in lysate APP holoprotein levels. Initially this result appears contradictory. However, an increase in APP holoprotein levels would not be observed if the protein was immediately processed by  $\alpha$ - and  $\beta$ - secretase. Therefore, these results suggest that Wt-APP overexpressing cells exhibited increased APP holoprotein levels with subsequently increased sAPP $\alpha$  levels with no resultant net detection of steady state holoprotein levels in cell lysates. A limit of transient transfection is that there is no antibiotic selection to ensure successful uptake of the constructs in all the cells analysed. It is, therefore, possible that the transient transfection of Wt-APP<sub>695</sub> was more successful than the APP-E2 CuBD mutants, leading to increased proteolysis and sAPP $\alpha$  generation within the short time frame involved.

Previous studies have implicated the APP-E1 CuBD in APP proteolysis. Spoerri *et al.* [117] mutated E1-CuBD binding residues to asparagine, which significantly decreased APP processing. In addition Borchardt *et al.* [98] demonstrated

that low levels of copper increase non-amyloidogenic processing which they further showed is abolished when the CuBD is mutated [123]. Taken with our results, these data support the E1 CuBD, rather than the E2 CuBD as a regulator of APP proteolysis. Recently our laboratory generated HEK and SH-SY5Y cells overexpressing APP E1-CuBD histidine to alanine mutations in the copper binding residues [124]. This mutation was considered conservative due to the helix-promoting properties of alanine. The E1-CuBD mutants failed to affect both the maturation and proteolysis of APP relative to Wt-APP, which suggests that, in conflict to Spoerri *et al* [117] the APP-E1 CuBD copper binding site is not implicated in APP processing. The disrupted APP processing observed in the E1 CuBD copper binding mutants generated by Spoerri *et al* [117] is likely a result of mutating histidine to asparagine, which due to its' helix breaking properties would induce significant conformational change in the protein. Therefore it currently appears that neither the E1 nor E2 copper binding site influence APP processing.

#### **4.1.3. APP localisation**

Nascent APP is trafficked along the secretory pathway to the cell surface, where it is quickly re-internalised to lysosomes where most is degraded [125]. Copper (150  $\mu$ M) has been shown to stimulate APP redistribution to the cell-surface, however the mechanism by which copper influences APP sub-localisation is unknown. As discussed previously, Dahms *et al.* [119] proposed that the copper induced conformational change observed in the APP-E2 CuBD may alter access for trafficking proteins such as Sor/La, subsequently regulating APP localisation. Therefore, one aim of the current project was to determine if mutating the APP-E2 CuBD altered APP sub-cellular localisation.

SH-SY5Y cells overexpressing the APP-E2 CuBD mutants or Wt-APP were subject to immunofluorescence confocal microscopy to detect APP subcellular localisation. This revealed a pronounced perinuclear localisation of APP. In the copper-free conditions employed in this study, mutating the copper binding residues of the APP-E2 CuBD did not alter APP subcellular localisation relative to Wt-APP overexpressing cells. A limitation of IF confocal microscopy is that, as a result of the whole cell being stained, there is increased risk of cross-reactivity compared to techniques that analyse specific cell fractions and this must be considered when interpreting results. Using a different primary antibody to stain for APP may reduce this problem.

Co-stains for organelle markers were not used for the comparison of APP localisation in this study. However, previous studies have utilised Golgi and ER markers to confirm the subcellular localisation of APP to a specific part of the constitutive secretory pathway [117]. Repeating this experiment with co-stains for organelle markers would further support the data obtained.

#### **4.1.4. Copper-mediated cytotoxicity**

As discussed in the introduction, high levels of copper are neurotoxic to cells. However, studies exploring the role of APP in response to copper are conflicting with evidence supporting both a neuroprotective function [102] and a role as a potentiator of copper induced cytotoxicity [35]. The final aim of the current project was, therefore, to determine if mutating the APP-E2 CuBD altered cytotoxicity in response to copper. HEK and SH-SY5Y cells stably transfected with the APP-E2 CuBD mutants or Wt-APP were incubated in a range of concentrations of free or glycine-

complexed copper. Following this a cell proliferation test was performed to quantify viability.

Initially, both HEK and SH-SY5Y cells were incubated in 'free' copper sulphate and viability was determined. In mock-transfected HEK cells, 50  $\mu\text{M}$  copper sulphate significantly enhanced cell viability to 117% relative to the copper-free control (Fig. 3.12). The average copper level in the neuropil of healthy individuals has been determined at  $\approx 79\mu\text{M}$  [104] suggesting that such a metal concentration is suitable for normal healthy cell function. Thus, in the current study, the increased cell viability observed at 50  $\mu\text{M}$  copper may be a consequence of the metal's involvement in essential cell enzyme function such as cytochrome c oxidase, lysyl oxidase, ceruloplasmin, superoxide dismutase and catechol oxidase activities [83]. However, the result appears cell line specific and was not replicated in SH-SY5Y cells.

Copper can accumulate in synaptic clefts to concentrations of  $\approx 100\ \mu\text{M}$  [126], and in A $\beta$  senile plaques to concentrations of  $\approx 400\ \mu\text{M}$  [104]. The concentrations used in the current study (50-600  $\mu\text{M}$ ) are within the same order of magnitude as these values and can, therefore, be considered of biological relevance. HEK cells overexpressing Wt-APP exhibited significantly reduced cell viability ( $\approx 15\%$ ) relative to the mock-transfected controls in the presence of 200  $\mu\text{M}$  copper sulphate and 600  $\mu\text{M}$  glycine-complexed metal. In addition, SH-SY5Y cells overexpressing Wt-APP exhibited reduced cell viability ( $\approx 13\%$ ) relative to mock-transfected controls in 600  $\mu\text{M}$  glycine-complexed copper. These data suggest that APP potentiates cytotoxicity in the presence of higher copper concentrations. These data are in agreement with White *et al.* [35] who determined a  $\approx 20\%$  reduction in viability in wild-type APP neurons compared with APP knock-out neurons in the presence of 100  $\mu\text{M}$  copper.

HEK cells overexpressing the APP-E2 CuBD mutants (with the exception of the H436A construct) did not demonstrate altered viability in the presence of copper relative to Wt-APP over-expressing cells. HEK cells transfected with the H436A construct exhibited significantly increased cell viability at both 250 and 600  $\mu\text{M}$  glycine-complexed copper relative to wild-type overexpressing cells. However, this observation was not duplicated in SH-SY5Y cells suggesting that it was cell line specific. Taken together, it appears from these data that the APP-E2 CuBD does not mediate the increased cytotoxicity observed in Wt-APP overexpressing cells.

APP may facilitate neurotoxicity through the increase of  $\text{A}\beta$  deposition.  $\text{A}\beta$  fibrils have previously been detected in cell medium after only a 24 h incubation [106]; the same time frame used in the current cytotoxicity experiments. It is, therefore, conceivable that the increased copper-mediated cytotoxicity observed in APP over-expressing cells in the current study was due to the enhanced accumulation of  $\text{A}\beta$ -peptides in conditioned medium. Indeed copper incubation increases  $\text{A}\beta$  oligomer/fibril ratio [106] and supplementing drinking water with copper in cholesterol fed rabbits induces amyloid plaques and learning deficits [127]. However other studies have shown that copper decreases the  $\text{A}\beta$ -42/ $\text{A}\beta$ -40 ratio and reduces  $\text{A}\beta$  generation [98], and results are often limited to specific species or cell lines [94].

Collectively, the current data indicates that the APP E2 CuBD is not involved in the ability of the protein to enhance metal-mediated cytotoxicity. Indeed this conclusion is supported by the work of Cerpa *et al.* [102] who concluded that the APP E1 CuBD was sufficient for the protective effect of APP-overexpression in increased copper concentrations -. Specifically, the authors showed that the reduced toxicity was due to the ability of Cys 144 within the APP molecule to reduce Cu (II) to Cu (I)

Interestingly, in the current study, SH-SY5Y cells seemed generally more resilient to copper-mediated cytotoxicity than HEK cells suggesting that the two cell types may have varying abilities to protect themselves against the metal. In fact, enhanced glutathione levels indicate that human neuron-related cells such as SH-SY5Y exhibit decreased anti-oxidant defence capability compared with cells derived from other tissues [128].

#### **4.2. Conclusions and future directions**

In summary, these data clearly show that the APP-E2 CuBD is not involved in APP maturation, processing or localisation in the absence of exogenous copper. Viability assays showed that APP overexpression is cytotoxic in increased copper concentrations; however the APP-E2 CuBD does not mediate this toxicity. Some of the cell-line specific results obtained from this project highlight the influence of cell line on data acquisition. Indeed, Cater *et al.* [94] found that the differences in APP proteolysis observed in copper deficient fibroblasts were not replicated in SH-SY5Y neuronal cells. To improve reliability of these data, experiments could be replicated in further cell lines.

One additional limitation of the current study was that the effects of exogenous copper on the expression and proteolysis of the various over-expressed constructs were not investigated. These experiments would be difficult to perform in the current cell models as both HEK and SH-SY5Y cells express quite high endogenous levels of APP which might confound the effects of copper on any transfected forms of APP. Expressing the constructs in APP null cells might overcome this issue in future studies.

## References

1. Duce, J.A., et al., *Iron-export ferroxidase activity of beta-amyloid precursor protein is inhibited by zinc in Alzheimer's disease*. Cell, 2010. **142**(6): p. 857-67.
2. Sleegers, K., et al., *The pursuit of susceptibility genes for Alzheimer's disease: progress and prospects*. Trends Genet, 2010. **26**(2): p. 84-93.
3. Guerreiro, R., et al., *TREM2 variants in Alzheimer's disease*. N Engl J Med, 2013. **368**(2): p. 117-27.
4. Lutsenko, S., et al., *Function and regulation of human copper-transporting ATPases*. Physiol Rev, 2007. **87**(3): p. 1011-46.
5. *2013 Alzheimer's disease facts and figures*. Alzheimer's & dementia : the journal of the Alzheimer's Association, 2013. **9**(2): p. 208-245.
6. Brookmeyer, R., et al., *Forecasting the global burden of Alzheimer's disease*. Alzheimer's & Dementia, 2007. **3**(3): p. 186 - 191.
7. Goedert, M. and M.G. Spillantini, *A Century of Alzheimer's Disease*. Science, 2006. **314**(5800): p. 777-781.
8. Blessed, G., B.E. Tomlinson, and M. Roth, *The Association Between Quantitative Measures of Dementia and of Senile Change in the Cerebral Grey Matter of Elderly Subjects*. The British Journal of Psychiatry, 1968. **114**(512): p. 797-811.
9. Serrano-Pozo, A., et al., *Neuropathological Alterations in Alzheimer Disease*. Cold Spring Harbor Perspectives in Medicine, 2011. **1**(1).
10. Wolfe, M.S., *The role of tau in neurodegenerative diseases and its potential as a therapeutic target*. Scientifica (Cairo), 2012. **2012**: p. 796024.
11. Bird, T.D., *Genetic aspects of Alzheimer disease*. Genetics in Medicine, 2008. **10**(4): p. 231-239.
12. Kaye, R., et al., *Common structure of soluble amyloid oligomers implies common mechanism of pathogenesis*. Science, 2003. **300**(5618): p. 486-9.
13. Hardy, J. and D.J. Selkoe, *The amyloid hypothesis of Alzheimer's disease: progress and problems on the road to therapeutics*. Science, 2002. **297**(5580): p. 353-6.
14. Robakis, N.K., *Are A $\beta$  and Its Derivatives Causative Agents or Innocent Bystanders in AD?* Neurodegener Dis, 2010. **7**(1-3): p. 32-7.
15. Castellani, R.J., et al., *PHOSPHORYLATED TAU: TOXIC, PROTECTIVE, OR NONE OF THE ABOVE*. J Alzheimers Dis, 2008. **14**(4): p. 377-83.
16. Gauthier, S., et al., *Mild cognitive impairment*. Lancet, 2006. **367**(9518): p. 1262-70.
17. Gabryelewicz, T., et al., *The rate of conversion of mild cognitive impairment to dementia: predictive role of depression*. Int J Geriatr Psychiatry, 2007. **22**(6): p. 563-7.
18. Reisberg, B., et al., *The Global Deterioration Scale for assessment of primary degenerative dementia*. The American Journal of Psychiatry, 1982. **139**(9): p. 1136-1139.
19. NICE, *CG42 Dementia: NICE guideline*. 2006, NICE: <http://publications.nice.org.uk/dementia-cg42/guidance#diagnosis-and-assessment-of-dementia>.
20. Hansen, R.A., et al., *Efficacy and safety of donepezil, galantamine, and rivastigmine for the treatment of Alzheimer's disease: a systematic review and meta-analysis*. Clin Interv Aging, 2008. **3**(2): p. 211-25.
21. Tayeb, H.O., et al., *Pharmacotherapies for Alzheimer's disease: beyond cholinesterase inhibitors*. Pharmacology and Therapeutics, 2012. **134**(1): p. 8-25.
22. Larson, E.B., et al., *Survival after initial diagnosis of Alzheimer disease*. Ann Intern Med, 2004. **140**(7): p. 501-9.
23. Humbert, I.A., et al., *Early deficits in cortical control of swallowing in Alzheimer's disease*. J Alzheimers Dis, 2010. **19**(4): p. 1185-97.
24. Beard, C.M., et al., *Cause of death in Alzheimer's disease*. Ann Epidemiol, 1996. **6**(3): p. 195-200.

25. de la Torre, J.C., *Is Alzheimer's disease a neurodegenerative or a vascular disorder? Data, dogma, and dialectics*. The Lancet Neurology, 2004. **3**(3): p. 184-190.
26. Zlokovic, B.V., *Neurovascular mechanisms of Alzheimer's neurodegeneration*. Trends in Neurosciences, 2005. **28**(4): p. 202-208.
27. Hofman, A., et al., *Atherosclerosis, apolipoprotein E, and prevalence of dementia and Alzheimer's disease in the Rotterdam Study*. Lancet, 1997. **349**(9046): p. 151-4.
28. Deane, R., et al., *LRP/amyloid beta-peptide interaction mediates differential brain efflux of A $\beta$  isoforms*. Neuron, 2004. **43**(3): p. 333-44.
29. Gong, C.X. and K. Iqbal, *Hyperphosphorylation of Microtubule-Associated Protein Tau: A Promising Therapeutic Target for Alzheimer Disease*. Curr Med Chem, 2008. **15**(23): p. 2321-8.
30. Roberson, E.D., et al., *Reducing endogenous tau ameliorates amyloid beta-induced deficits in an Alzheimer's disease mouse model*. Science, 2007. **316**(5825): p. 750-4.
31. Craddock, T.J., et al., *The zinc dyshomeostasis hypothesis of Alzheimer's disease*. PLoS One, 2012. **7**(3): p. e33552.
32. Markesbery, W.R., *Oxidative stress hypothesis in Alzheimer's disease*. Free Radic Biol Med, 1997. **23**(1): p. 134-47.
33. Pratico, D., *Oxidative stress hypothesis in Alzheimer's disease: a reappraisal*. Trends Pharmacol Sci, 2008. **29**(12): p. 609-15.
34. Zhu, X., et al., *Oxidative stress signalling in Alzheimer's disease*. Brain Res, 2004. **1000**(1-2): p. 32-9.
35. White, A.R., et al., *The Alzheimer's disease amyloid precursor protein modulates copper-induced toxicity and oxidative stress in primary neuronal cultures*. J Neurosci, 1999. **19**(21): p. 9170-9.
36. Sano, M., et al., *A controlled trial of selegiline, alpha-tocopherol, or both as treatment for Alzheimer's disease. The Alzheimer's Disease Cooperative Study*. N Engl J Med, 1997. **336**(17): p. 1216-22.
37. Tanzi, R.E. and L. Bertram, *New frontiers in Alzheimer's disease genetics*. Neuron, 2001. **32**(2): p. 181-4.
38. Townsend, M., et al., *Effects of secreted oligomers of amyloid  $\beta$ -protein on hippocampal synaptic plasticity: a potent role for trimers*. J Physiol, 2006. **572**(Pt 2): p. 477-92.
39. Lambert, M.P., et al., *Diffusible, nonfibrillar ligands derived from A $\beta$ 1-42 are potent central nervous system neurotoxins*. Proc Natl Acad Sci U S A, 1998. **95**(11): p. 6448-53.
40. White, J.A., et al., *Differential effects of oligomeric and fibrillar amyloid-beta 1-42 on astrocyte-mediated inflammation*. Neurobiol Dis, 2005. **18**(3): p. 459-65.
41. Dahlgren, K.N., et al., *Oligomeric and fibrillar species of amyloid-beta peptides differentially affect neuronal viability*. J Biol Chem, 2002. **277**(35): p. 32046-53.
42. Kumar-Singh, S., et al., *Mean age-of-onset of familial alzheimer disease caused by presenilin mutations correlates with both increased A $\beta$ 42 and decreased A $\beta$ 40*. Hum Mutat, 2006. **27**(7): p. 686-95.
43. Cummings, B.J., et al., *Beta-amyloid deposition and other measures of neuropathology predict cognitive status in Alzheimer's disease*. Neurobiol Aging, 1996. **17**(6): p. 921-33.
44. Goate, A., et al., *Segregation of a missense mutation in the amyloid precursor protein gene with familial Alzheimer's disease*. Nature, 1991. **349**(6311): p. 704-6.
45. De Jonghe, C., et al., *Pathogenic APP mutations near the gamma-secretase cleavage site differentially affect A $\beta$  secretion and APP C-terminal fragment stability*. Hum Mol Genet, 2001. **10**(16): p. 1665-71.

46. Muratore, C.R., et al., *The familial Alzheimer's disease APPV717I mutation alters APP processing and Tau expression in iPSC-derived neurons*. Hum Mol Genet, 2014. **23**(13): p. 3523-36.
47. Thinakaran, G., et al., *Endoproteolysis of presenilin 1 and accumulation of processed derivatives in vivo*. Neuron, 1996. **17**(1): p. 181-90.
48. Bertram, L., C.M. Lill, and R.E. Tanzi, *The genetics of Alzheimer disease: back to the future*. Neuron, 2010. **68**(2): p. 270-81.
49. Kang, J., et al., *The precursor of Alzheimer's disease amyloid A4 protein resembles a cell-surface receptor*. Nature, 1987. **325**(6106): p. 733-6.
50. O'Brien, R.J. and P.C. Wong, *Amyloid precursor protein processing and Alzheimer's disease*. Annu Rev Neurosci, 2011. **34**: p. 185-204.
51. Sisodia, S., Koo, EH, et al., *Identification and transport of full-length amyloid precursor proteins in rat peripheral nervous system*. The Journal of Neuroscience, 1993. **13**(7): p. 3136-3142.
52. Müller, U.C. and H. Zheng, *Physiological Functions of APP Family Proteins*. Cold Spring Harbor Perspectives in Medicine, 2012. **2**(2).
53. Roch, J.M., et al., *Increase of synaptic density and memory retention by a peptide representing the trophic domain of the amyloid beta/A4 protein precursor*. Proc Natl Acad Sci U S A, 1994. **91**(16): p. 7450-4.
54. Walter, J. and C. Haass, *Posttranslational modifications of amyloid precursor protein : ectodomain phosphorylation and sulfation*. Methods Mol Med, 2000. **32**: p. 149-68.
55. Haass, C., et al., *Targeting of cell-surface beta-amyloid precursor protein to lysosomes: alternative processing into amyloid-bearing fragments*. Nature, 1992. **357**(6378): p. 500-3.
56. Zhang, Y.-w., et al., *APP processing in Alzheimer's disease*. Molecular Brain, 2011. **4**(1): p. 3.
57. Cheng, H., et al., *Mechanisms of Disease: new therapeutic strategies for Alzheimer's disease--targeting amyloid precursor protein processing in lipid rafts*. Nat Clin Pract Neurol, 2007. **3**(7): p. 374-82.
58. Vassar, R., et al., *Beta-secretase cleavage of Alzheimer's amyloid precursor protein by the transmembrane aspartic protease BACE*. Science, 1999. **286**(5440): p. 735-41.
59. Sinha, S., et al., *Purification and cloning of amyloid precursor protein beta-secretase from human brain*. Nature, 1999. **402**(6761): p. 537-40.
60. Yan, R., et al., *Membrane-anchored aspartyl protease with Alzheimer's disease beta-secretase activity*. Nature, 1999. **402**(6761): p. 533-7.
61. Cai, H., et al., *BACE1 is the major beta-secretase for generation of Abeta peptides by neurons*. Nat Neurosci, 2001. **4**(3): p. 233-4.
62. Kimberly, W.T., et al., *Gamma-secretase is a membrane protein complex comprised of presenilin, nicastrin, Aph-1, and Pen-2*. Proc Natl Acad Sci U S A, 2003. **100**(11): p. 6382-7.
63. Kaether, C., et al., *Amyloid precursor protein and Notch intracellular domains are generated after transport of their precursors to the cell surface*. Traffic, 2006. **7**(4): p. 408-15.
64. Gaus, K., et al., *Visualizing lipid structure and raft domains in living cells with two-photon microscopy*. Proc Natl Acad Sci U S A, 2003. **100**(26): p. 15554-9.
65. Pike, L.J., et al., *Lipid rafts are enriched in arachidonic acid and plasmenylethanolamine and their composition is independent of caveolin-1 expression: a quantitative electrospray ionization/mass spectrometric analysis*. Biochemistry, 2002. **41**(6): p. 2075-88.
66. Chia, P.Z. and P.A. Gleeson, *Intracellular trafficking of the beta-secretase and processing of amyloid precursor protein*. IUBMB Life, 2011. **63**(9): p. 721-9.

67. Roberts, S.B., et al., *Non-amyloidogenic cleavage of the beta-amyloid precursor protein by an integral membrane metalloendopeptidase*. J Biol Chem, 1994. **269**(4): p. 3111-6.
68. Lammich, S., et al., *Constitutive and regulated alpha-secretase cleavage of Alzheimer's amyloid precursor protein by a disintegrin metalloprotease*. Proc Natl Acad Sci U S A, 1999. **96**(7): p. 3922-7.
69. Postina, R., et al., *A disintegrin-metalloproteinase prevents amyloid plaque formation and hippocampal defects in an Alzheimer disease mouse model*. J Clin Invest, 2004. **113**(10): p. 1456-64.
70. Colciaghi, F., et al.,  *$\alpha$ -Secretase ADAM10 as well as  $\alpha$ APPs is reduced in platelets and CSF of Alzheimer disease patients*. Mol Med, 2002. **8**(2): p. 67-74.
71. Sisodia, S.S., *Beta-amyloid precursor protein cleavage by a membrane-bound protease*. Proc Natl Acad Sci U S A, 1992. **89**(13): p. 6075-9.
72. Small, D.H., et al., *A heparin-binding domain in the amyloid protein precursor of Alzheimer's disease is involved in the regulation of neurite outgrowth*. J Neurosci, 1994. **14**(4): p. 2117-27.
73. Breen, K.C., *APP-collagen interaction is mediated by a heparin bridge mechanism*. Mol Chem Neuropathol, 1992. **16**(1-2): p. 109-21.
74. Kibbey, M.C., et al., *beta-Amyloid precursor protein binds to the neurite-promoting IKVAV site of laminin*. Proc Natl Acad Sci U S A, 1993. **90**(21): p. 10150-3.
75. Soba, P., et al., *Homo- and heterodimerization of APP family members promotes intercellular adhesion*. Embo J, 2005. **24**(20): p. 3624-34.
76. Perez, R.G., et al., *The beta-amyloid precursor protein of Alzheimer's disease enhances neuron viability and modulates neuronal polarity*. J Neurosci, 1997. **17**(24): p. 9407-14.
77. Wang, P., et al., *Defective neuromuscular synapses in mice lacking amyloid precursor protein (APP) and APP-Like protein 2*. J Neurosci, 2005. **25**(5): p. 1219-25.
78. Herms, J., et al., *Cortical dysplasia resembling human type 2 lissencephaly in mice lacking all three APP family members*. EMBO J, 2004. **23**(20): p. 4106-15.
79. Hartl, D., Klatt, S., Roch, M., Konthur, Z., Klose, J., Willnow, T.E., Rohe, M., *Soluble Alpha-APP (sAPPalpha) Regulates CDK5 Expression and Activity in Neurons*. PLOS one, 2013. **8**(6): p. e65920.
80. Pardossi-Piquard, R. and F. Checler, *The physiology of the beta-amyloid precursor protein intracellular domain AICD*. J Neurochem, 2012. **120** Suppl 1: p. 109-24.
81. Konietzko, U., et al., *Co-localization of the amyloid precursor protein and the Notch intracellular domains in nuclear transcription factories*. Neurobiol Aging, 2010. **31**(1): p. 58-73.
82. Puzzo, D., et al., *Picomolar amyloid-beta positively modulates synaptic plasticity and memory in hippocampus*. J Neurosci, 2008. **28**(53): p. 14537-45.
83. Uauy, R., M. Olivares, and M. Gonzalez, *Essentiality of copper in humans*. Am J Clin Nutr, 1998. **67**(5 Suppl): p. 952s-959s.
84. Tapiero, H., Townsend, D.M., Tew, K.D., *Trace elements in human physiology and pathology. Copper*. Biomedicine & Pharmacotherapy, 2003. **57**(9): p. 386-398.
85. Bush, A.I., *The metallobiology of Alzheimer's disease*. Trends Neurosci, 2003. **26**(4): p. 207-14.
86. Eskici, G. and P.H. Axelsen, *Copper and Oxidative Stress in the Pathogenesis of Alzheimer's Disease*. Biochemistry, 2012. **51**(32): p. 6289-6311.
87. Linder, M.C., *Copper and genomic stability in mammals*. Mutat Res, 2001. **475**(1-2): p. 141-52.
88. de Bie, P., et al., *Molecular pathogenesis of Wilson and Menkes disease: correlation of mutations with molecular defects and disease phenotypes*, in J Med Genet. 2007. p. 673-88.

89. Pajonk, F.G., et al., *Cognitive decline correlates with low plasma concentrations of copper in patients with mild to moderate Alzheimer's disease*. J Alzheimers Dis, 2005. **8**(1): p. 23-7.
90. Smorgon, C., et al., *Trace elements and cognitive impairment: an elderly cohort study*. Arch Gerontol Geriatr Suppl, 2004. **2004**(9): p. 393-402.
91. Bucossi, S., et al., *Copper in Alzheimer's disease: a meta-analysis of serum, plasma, and cerebrospinal fluid studies*. J Alzheimers Dis, 2011. **24**(1): p. 175-85.
92. Deibel, M.A., Ehmann, W.D., Markesbury, W.R., *Copper, iron, and zinc imbalances in severely degenerated brain regions in Alzheimer's disease: possible relation to oxidative stress*. Journal of the Neurological Sciences, 1996. **143**(Issues 1–2): p. 137–142.
93. Religa, D., et al., *Elevated cortical zinc in Alzheimer disease*. Neurology, 2006. **67**(1): p. 69-75.
94. Cater, M.A., et al., *Intracellular copper deficiency increases amyloid-beta secretion by diverse mechanisms*. Biochem J, 2008. **412**(1): p. 141-52.
95. Armendariz, A.D., et al., *Gene expression profiling in chronic copper overload reveals upregulation of Prnp and App*. Physiol Genomics, 2004. **20**(1): p. 45-54.
96. Bellingham, S.A., et al., *Copper depletion down-regulates expression of the Alzheimer's disease amyloid-beta precursor protein gene*. J Biol Chem, 2004. **279**(19): p. 20378-86.
97. White, A.R., et al., *Copper levels are increased in the cerebral cortex and liver of APP and APLP2 knockout mice*. Brain Res, 1999. **842**(2): p. 439-44.
98. Borchardt, T., et al., *Copper inhibits beta-amyloid production and stimulates the non-amyloidogenic pathway of amyloid-precursor-protein secretion*. Biochem J, 1999. **344 Pt 2**: p. 461-7.
99. Acevedo, K.M., et al., *Copper promotes the trafficking of the amyloid precursor protein*. J Biol Chem, 2011. **286**(10): p. 8252-62.
100. Hung, Y.H., et al., *Paradoxical condensation of copper with elevated beta-amyloid in lipid rafts under cellular copper deficiency conditions: implications for Alzheimer disease*. J Biol Chem, 2009. **284**(33): p. 21899-907.
101. Multhaup, G., et al., *The amyloid precursor protein of Alzheimer's disease in the reduction of copper(II) to copper(I)*. Science, 1996. **271**(5254): p. 1406-9.
102. Cerpa, W.F., et al., *The N-terminal copper-binding domain of the amyloid precursor protein protects against Cu<sup>2+</sup> neurotoxicity in vivo*. Faseb J, 2004. **18**(14): p. 1701-3.
103. White, A.R., et al., *Contrasting, species-dependent modulation of copper-mediated neurotoxicity by the Alzheimer's disease amyloid precursor protein*. J Neurosci, 2002. **22**(2): p. 365-76.
104. Lovell, M.A., et al., *Copper, iron and zinc in Alzheimer's disease senile plaques*. J Neurol Sci, 1998. **158**(1): p. 47-52.
105. Huang, X., et al., *Trace metal contamination initiates the apparent auto-aggregation, amyloidosis, and oligomerization of Alzheimer's Aβ peptides*. J Biol Inorg Chem, 2004. **9**(8): p. 954-60.
106. Innocenti, M., et al., *Trace copper(II) or zinc(II) ions drastically modify the aggregation behavior of amyloid-beta<sub>1-42</sub>: an AFM study*. J Alzheimers Dis, 2010. **19**(4): p. 1323-9.
107. Curtain, C.C., et al., *Alzheimer's disease amyloid-beta binds copper and zinc to generate an allosterically ordered membrane-penetrating structure containing superoxide dismutase-like subunits*. J Biol Chem, 2001. **276**(23): p. 20466-73.
108. Jiang, D., et al., *The elevated copper binding strength of amyloid-beta aggregates allows the sequestration of copper from albumin: a pathway to accumulation of copper in senile plaques*. Biochemistry, 2013. **52**(3): p. 547-56.

109. Singh, I., et al., *Low levels of copper disrupt brain amyloid-beta homeostasis by altering its production and clearance*. Proc Natl Acad Sci U S A, 2013. **110**(36): p. 14771-6.
110. Butterfield, D.A., et al., *Evidence of oxidative damage in Alzheimer's disease brain: central role for amyloid beta-peptide*. Trends Mol Med, 2001. **7**(12): p. 548-54.
111. Eskici, G. and P.H. Axelsen, *Copper and oxidative stress in the pathogenesis of Alzheimer's disease*. Biochemistry, 2012. **51**(32): p. 6289-311.
112. Huang, X., et al., *The A beta peptide of Alzheimer's disease directly produces hydrogen peroxide through metal ion reduction*. Biochemistry, 1999. **38**(24): p. 7609-16.
113. Huang, X., et al., *Cu(II) potentiation of alzheimer abeta neurotoxicity. Correlation with cell-free hydrogen peroxide production and metal reduction*. J Biol Chem, 1999. **274**(52): p. 37111-6.
114. Allsop, D., et al., *Metal-dependent generation of reactive oxygen species from amyloid proteins implicated in neurodegenerative disease*. Biochem Soc Trans, 2008. **36**(Pt 6): p. 1293-8.
115. Kong, G.K., et al., *Structural studies of the Alzheimer's amyloid precursor protein copper-binding domain reveal how it binds copper ions*. J Mol Biol, 2007. **367**(1): p. 148-61.
116. Kong, G.K.W., et al., *Copper binding to the Alzheimer's disease amyloid precursor protein*. Eur Biophys J, 2008. **37**(3): p. 269-79.
117. Spoerri, L., et al., *The amyloid precursor protein copper binding domain histidine residues 149 and 151 mediate APP stability and metabolism*. J Biol Chem, 2012. **287**(32): p. 26840-53.
118. J.M, B., J.L. Tymoczko, and L. Stryer, *The Amino Acid Sequence of a Protein Determines Its Three-Dimensional Structure*. 2002, New York: W H Freeman.
119. Dahms, S.O., et al., *Metal Binding Dictates Conformation and Function of the Amyloid Precursor Protein (APP) E2 Domain*. Journal of Molecular Biology, 2012. **416**(3): p. 438 - 452.
120. Parkin, E.T., et al., *Cellular prion protein regulates beta-secretase cleavage of the Alzheimer's amyloid precursor protein*. Proc Natl Acad Sci U S A, 2007. **104**(26): p. 11062-7.
121. Agholme, L., et al., *An in vitro model for neuroscience: differentiation of SH-SY5Y cells into cells with morphological and biochemical characteristics of mature neurons*. J Alzheimers Dis, 2010. **20**(4): p. 1069-82.
122. Caughey, B. and P.T. Lansbury, *Protofibrils, pores, fibrils, and neurodegeneration: separating the responsible protein aggregates from the innocent bystanders*. Annu Rev Neurosci, 2003. **26**: p. 267-98.
123. Borchardt, T., Schmidt, C., Camarkis, J., Cappai, R., Masters, CL., Beyreuther, K., Multhaup, G., *Differential effects of zinc on amyloid precursor protein (APP) processing in copper-resistant variants of cultured Chinese hamster ovary cells*. Cell Mol Biol (Noisy-le-grand). 2000. **46**(4): p. 785-795.
124. Gough, M., S. Blanthorn-Hazell, and E.T. Parkin, *The Histidine Composition of the Amyloid-beta Domain, but not the E1 Copper Binding Domain, Modulates beta-Secretase Processing of Amyloid-beta Protein Precursor in Alzheimer's Disease*. J Alzheimers Dis, 2014.
125. Thinakaran, G., Koo, EH., *Amyloid Precursor Protein Trafficking, Processing, and Function*. The Journal of Biological Chemistry, 2008. **283**: p. 29615-29619.
126. Kardos, J., et al., *Nerve endings from rat brain tissue release copper upon depolarization. A possible role in regulating neuronal excitability*. Neurosci Lett, 1989. **103**(2): p. 139-44.

127. Sparks, D.L. and B.G. Schreurs, *Trace amounts of copper in water induce beta-amyloid plaques and learning deficits in a rabbit model of Alzheimer's disease*. Proc Natl Acad Sci U S A, 2003. **100**(19): p. 11065-9.
128. Slivka, A., M.B. Spina, and G. Cohen, *Reduced and oxidized glutathione in human and monkey brain*. Neurosci Lett, 1987. **74**(1): p. 112-8.